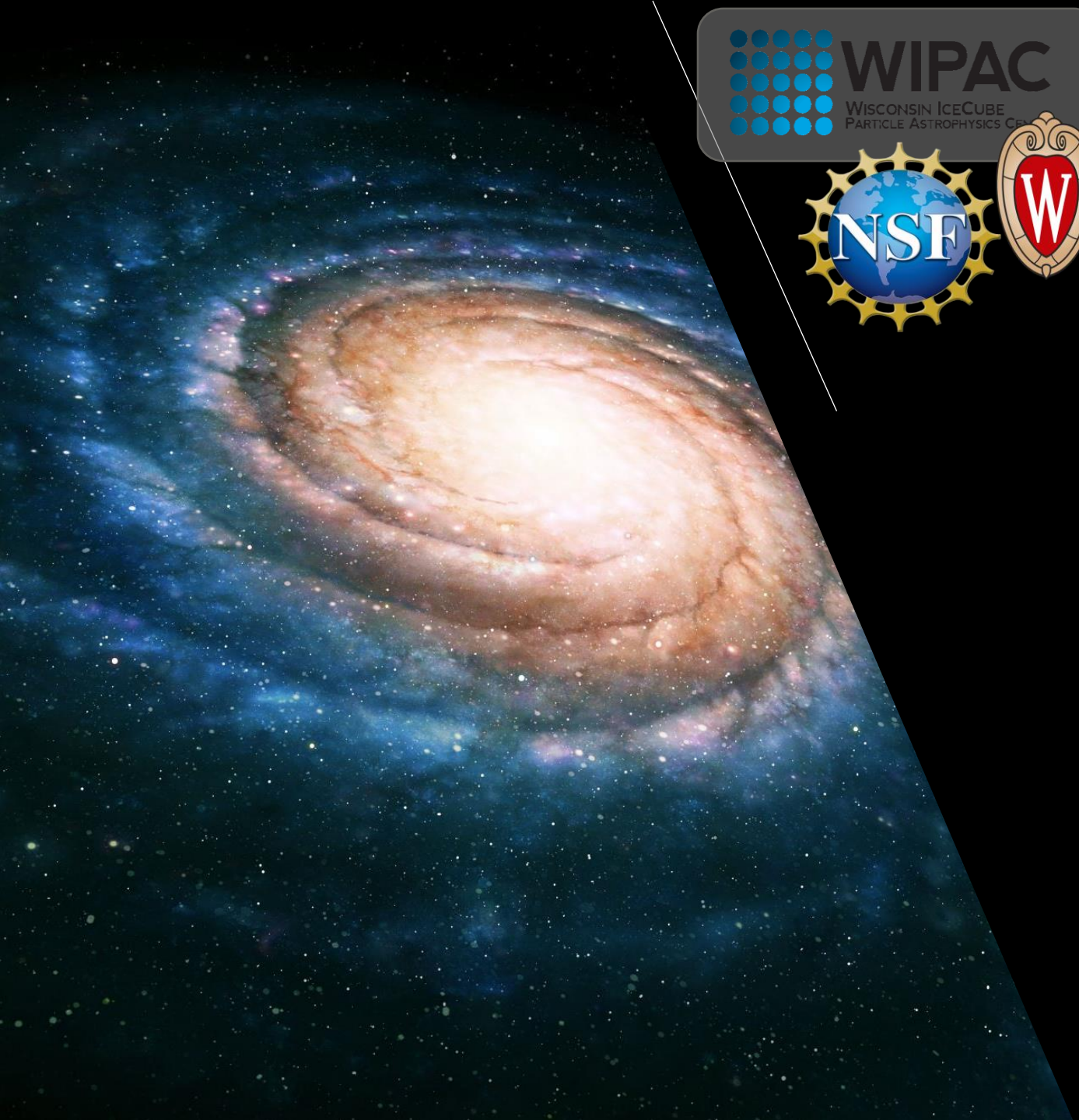

CONSTRAINING GALACTIC COSMIC RAY MODELS WITH A MULTI-MESSENGER ANALYSIS OF DIFFUSE EMISSION

Alisha Roberts[1], Dan Hooper[1], Ilias Cholis[2], Samyak Jain[1]

[1]University of Wisconsin-Madison, [2]Oakland University

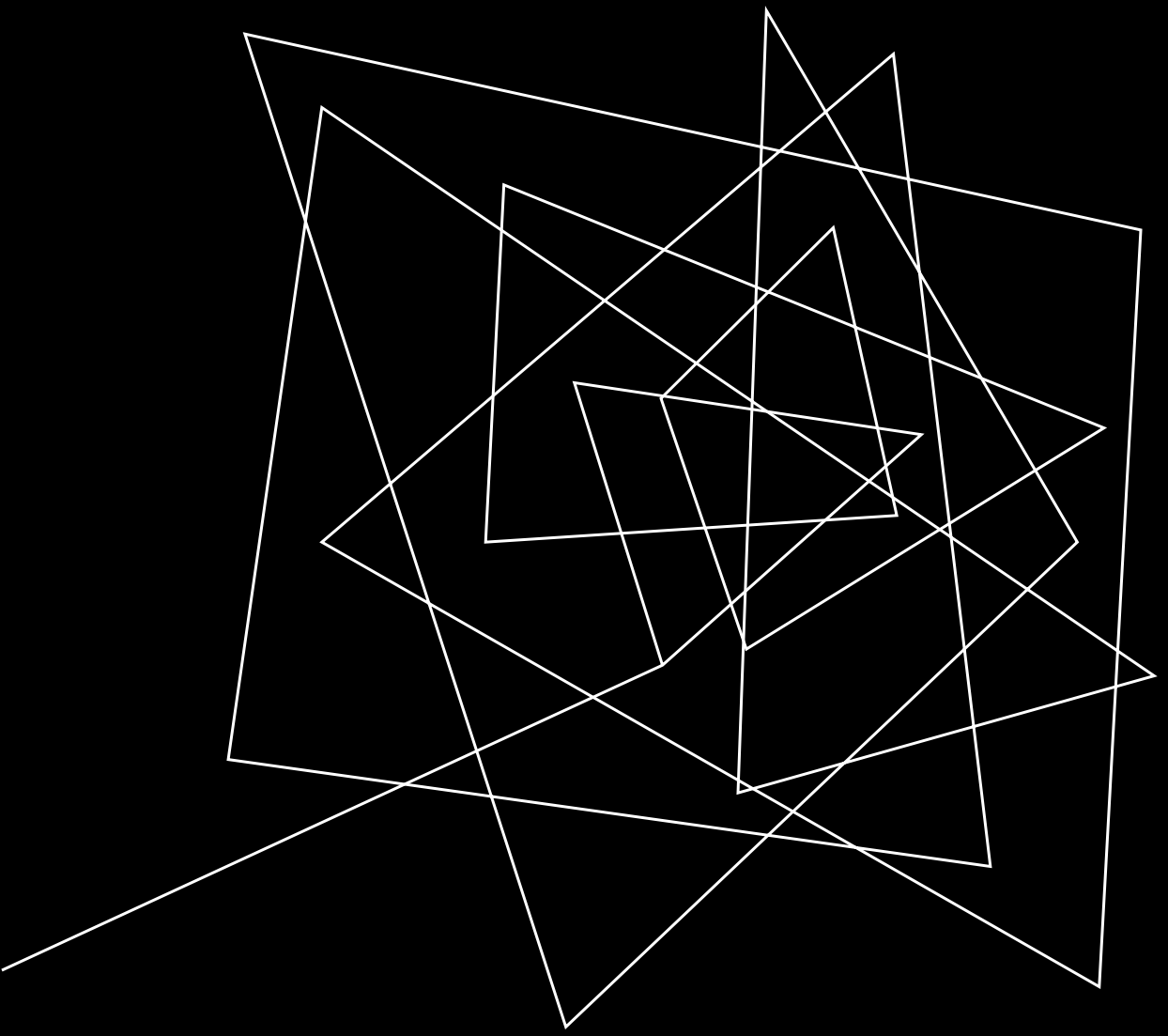

BACKGROUND

Cosmic Rays

Highly energetic particles

IceCube Collaboration (2012). *Rendering of cosmic rays hitting Earth.*

Galactic

Cosmic Rays

Highly energetic particles

Spectrum by galactic sources generally defined by power-law

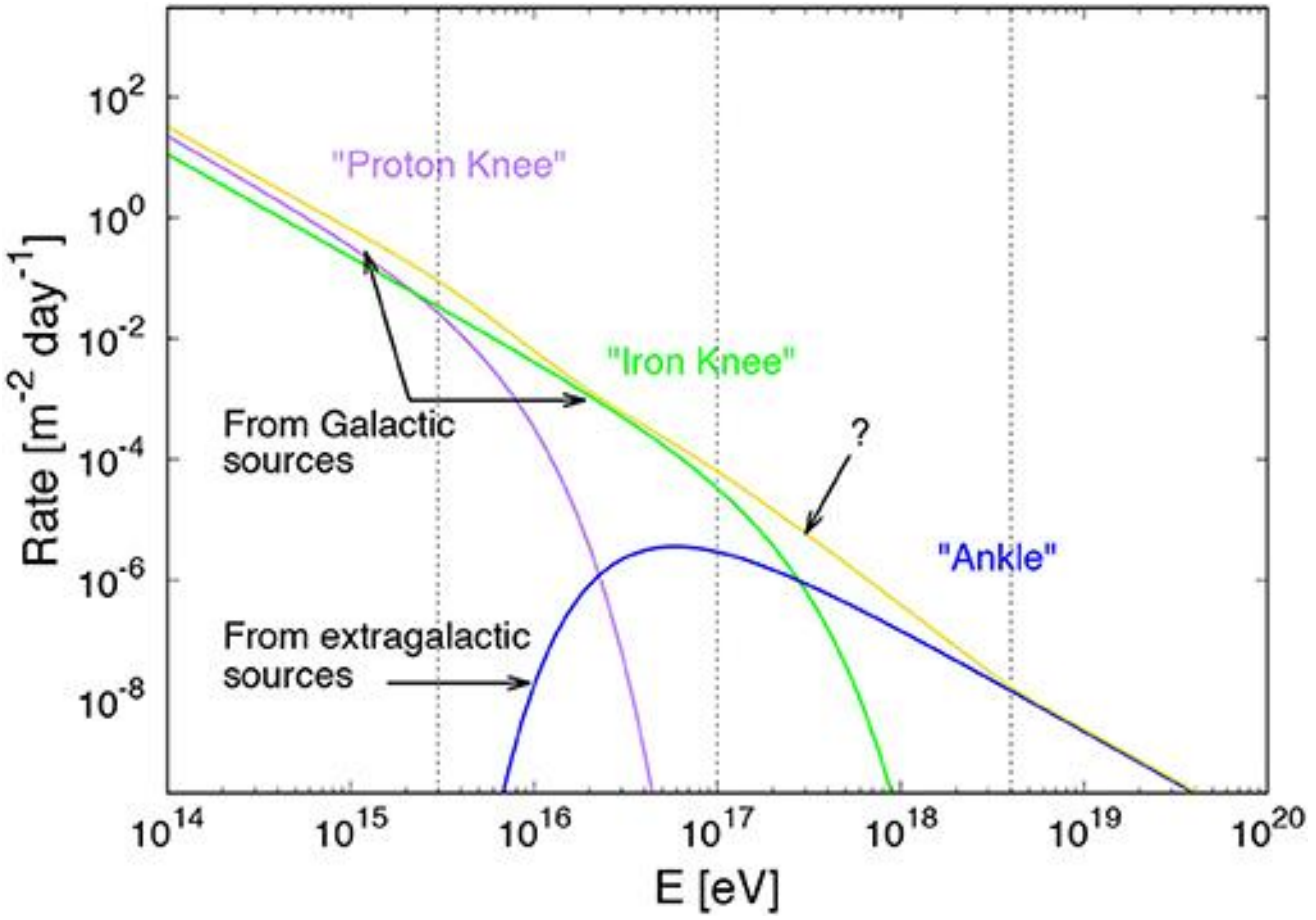

Rafael, R., et. Al. (2019). *Open Questions in Cosmic-Ray Research at Ultrahigh Energies*. Frontiers in Astronomy and Space Sciences.

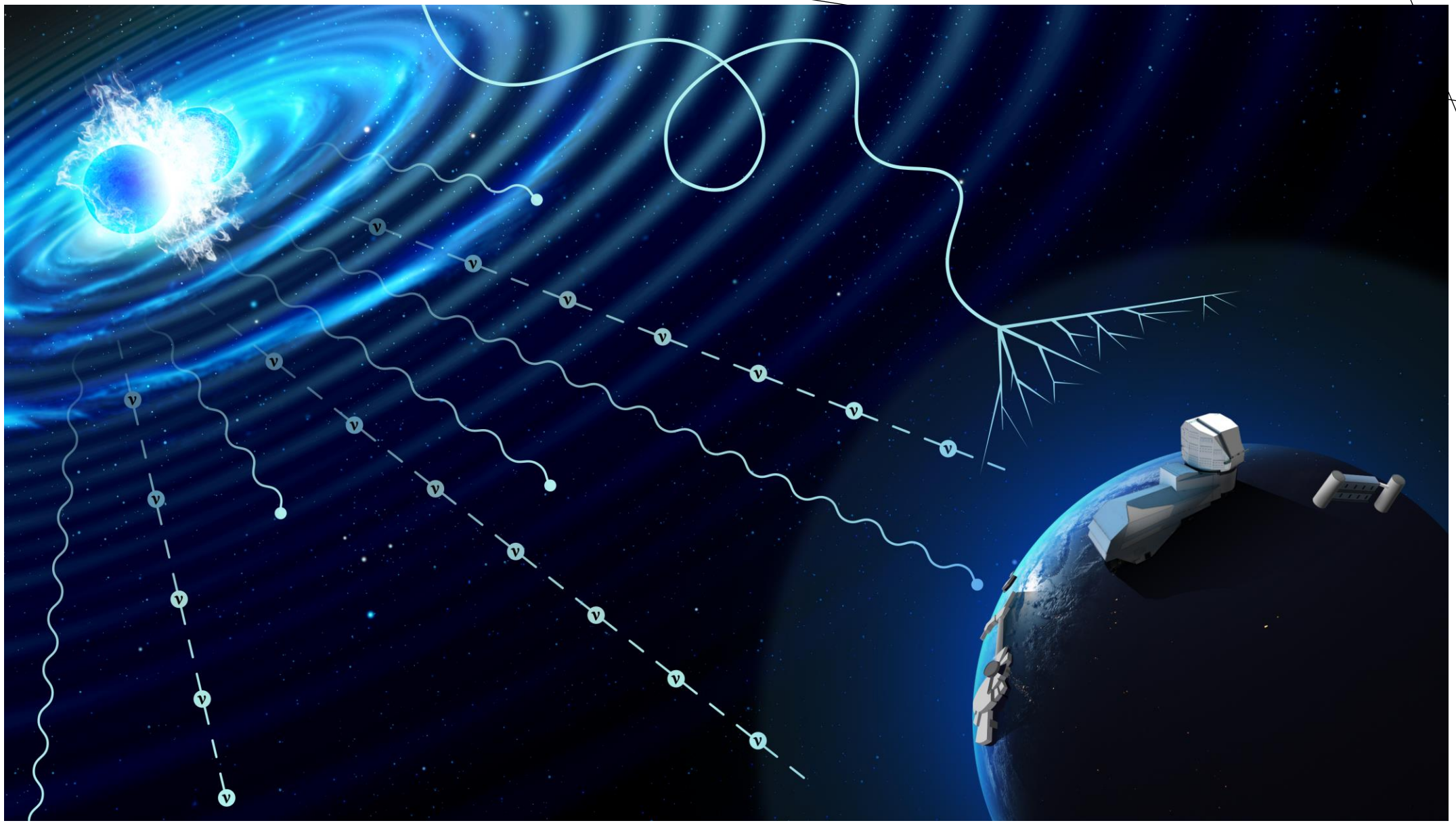

RubinObs/NOIRLab/SLAC/NSF/DOE/AURA/P. Marenfeld (2024). *Artist's Illustration of Multi-Messenger Event*

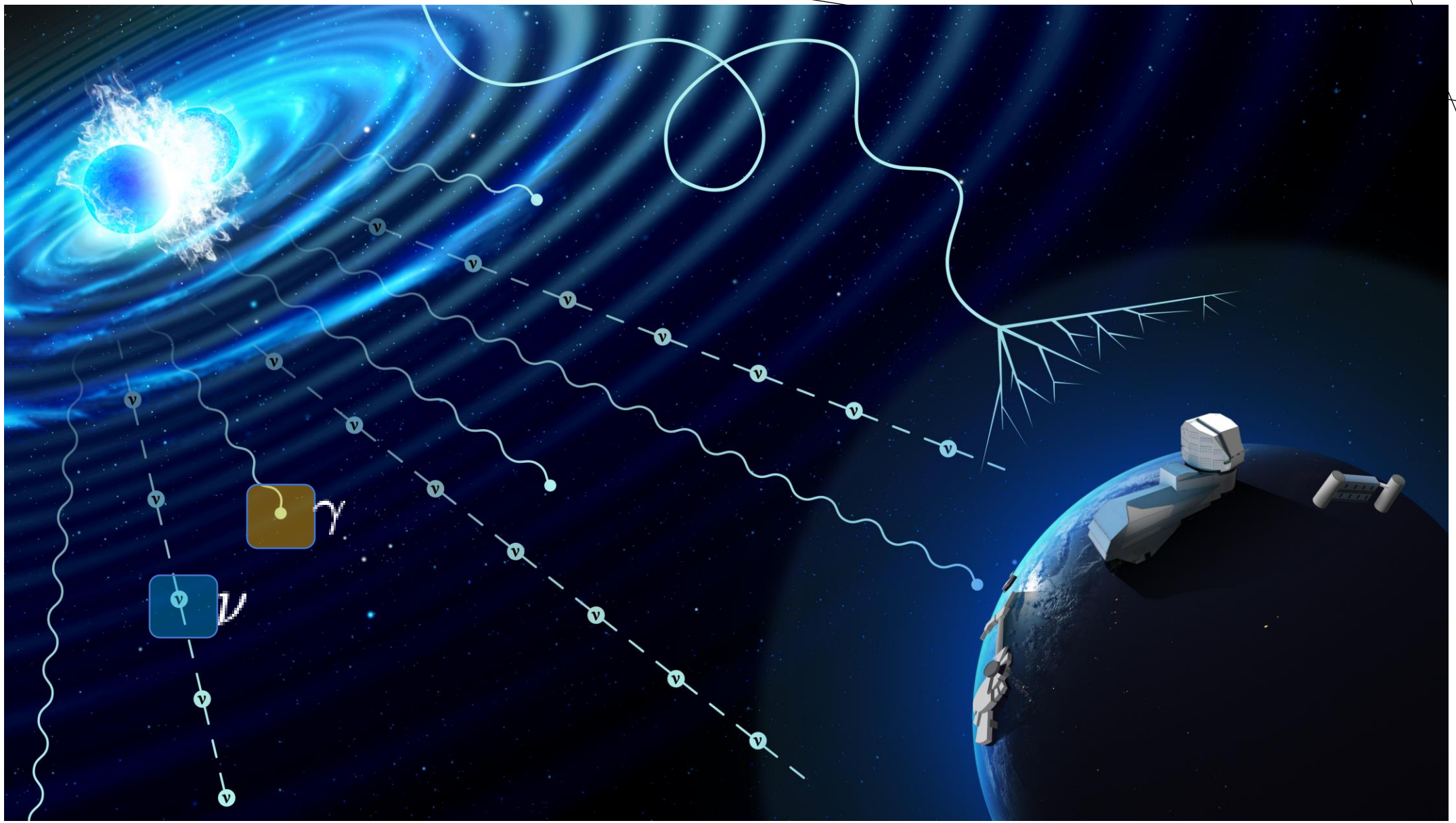

RubinObs/NOIRLab/SLAC/NSF/DOE/AURA/P. Marenfeld (2024). *Artist's Illustration of Multi-Messenger Event*

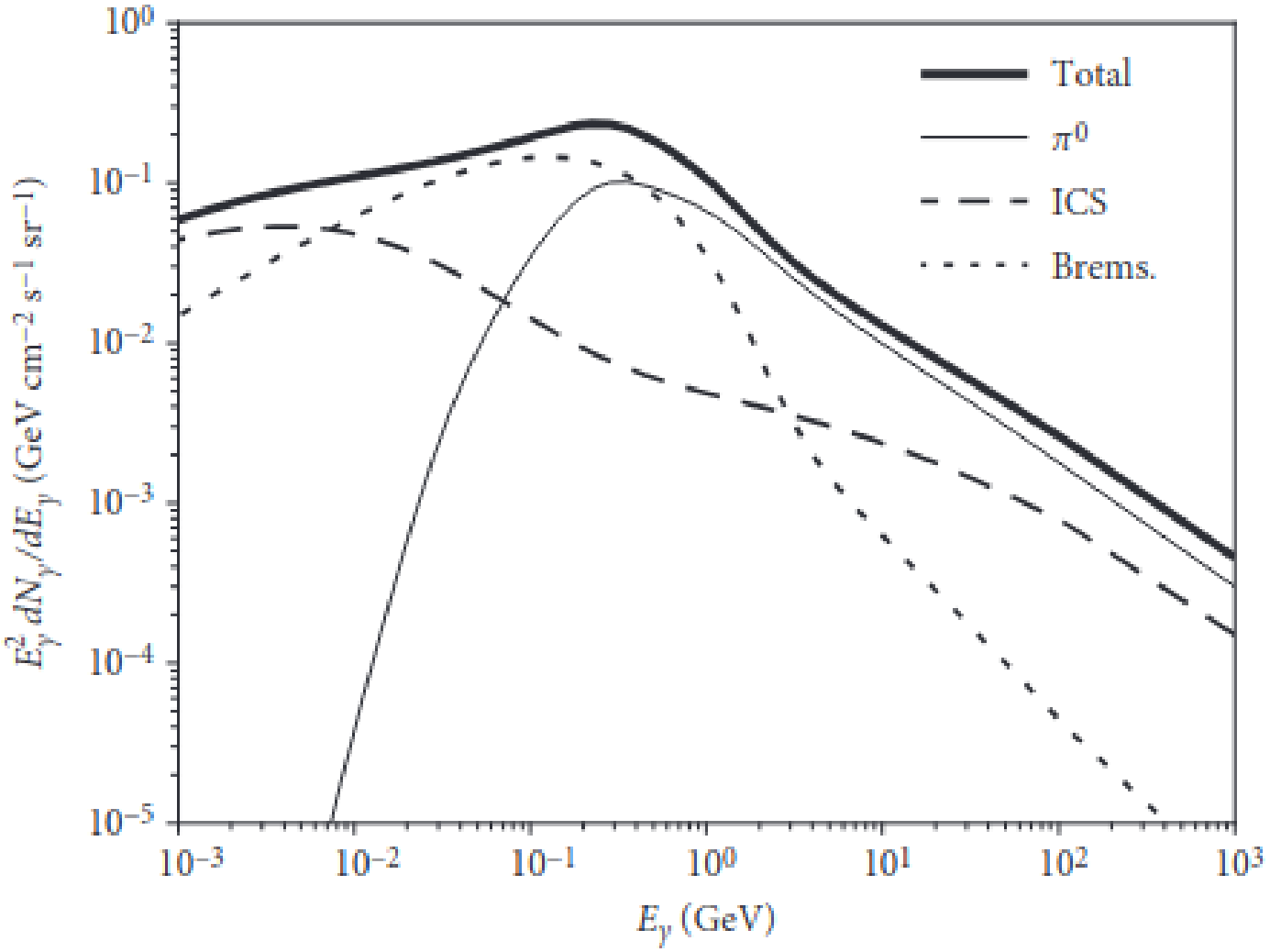

Hooper, D. (2024). *Particle Cosmology and Astrophysics.* Princeton University Press.

Gamma-rays

Produced in high-energy interactions, often linked with the decay of neutral pions from interacting cosmic rays

✚ Trace regions where high energy particles are interacting

▬ Produced both leptonically and hadronically

Gamma-rays

via Bremsstrahlung

traces high-energy
electrons in dense gas

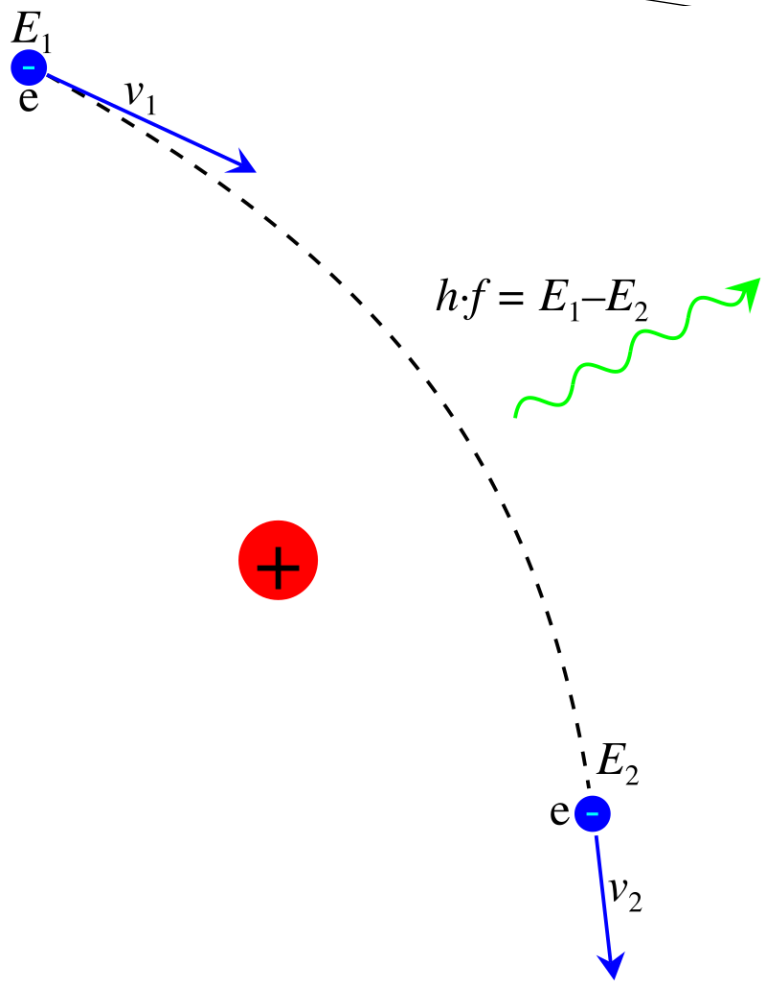

Martin, Dylan (2005). *X-Ray Detection*. University of Arizona Optical Sciences Center

Gamma-rays

Leptonic

via Bremsstrahlung

via Inverse Compton Scattering

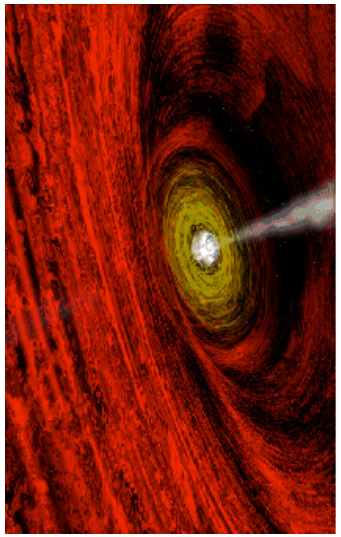

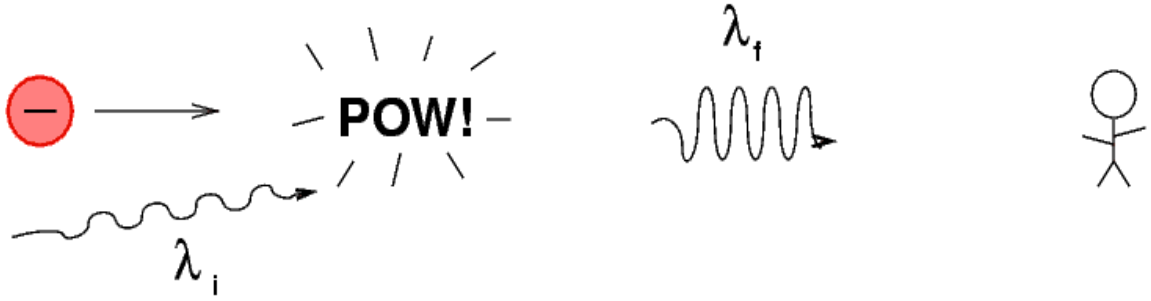

high-energy (relativistic) electron (e.g., supernovae remnant) transfers energy to low-energy photon (CMB/starlight)

Richmond, M. (2005) *PHYS 314 Lecture on ICS*. Rochester Institute of Technology

Gamma-rays

Leptonic

via Bremsstrahlung

via Inverse Compton Scattering

Hadronic

via Neutral Pion Decay

$$p + p_{\mathrm{ISM}} \rightarrow p + p + \pi^0 \rightarrow p + p + \gamma\gamma$$

Main channel of production

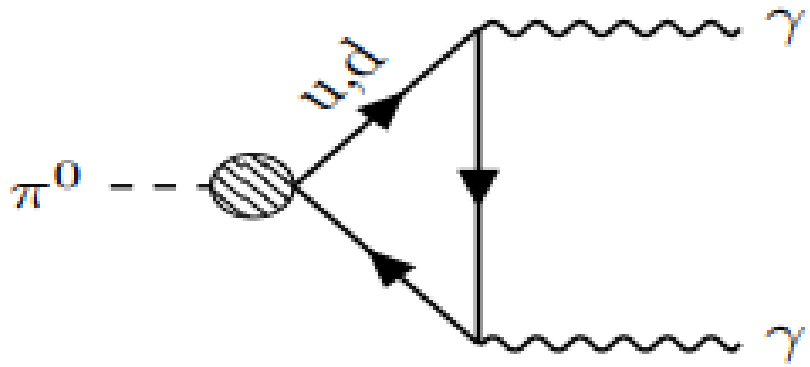

Bryman, D., Shrock, R. (2025) *Feynman Diagram of Neutral Pion Decay*. arXiv:2502.18384

TeV Halos: young and middle-aged pulsars glow brightly in TeV gamma rays

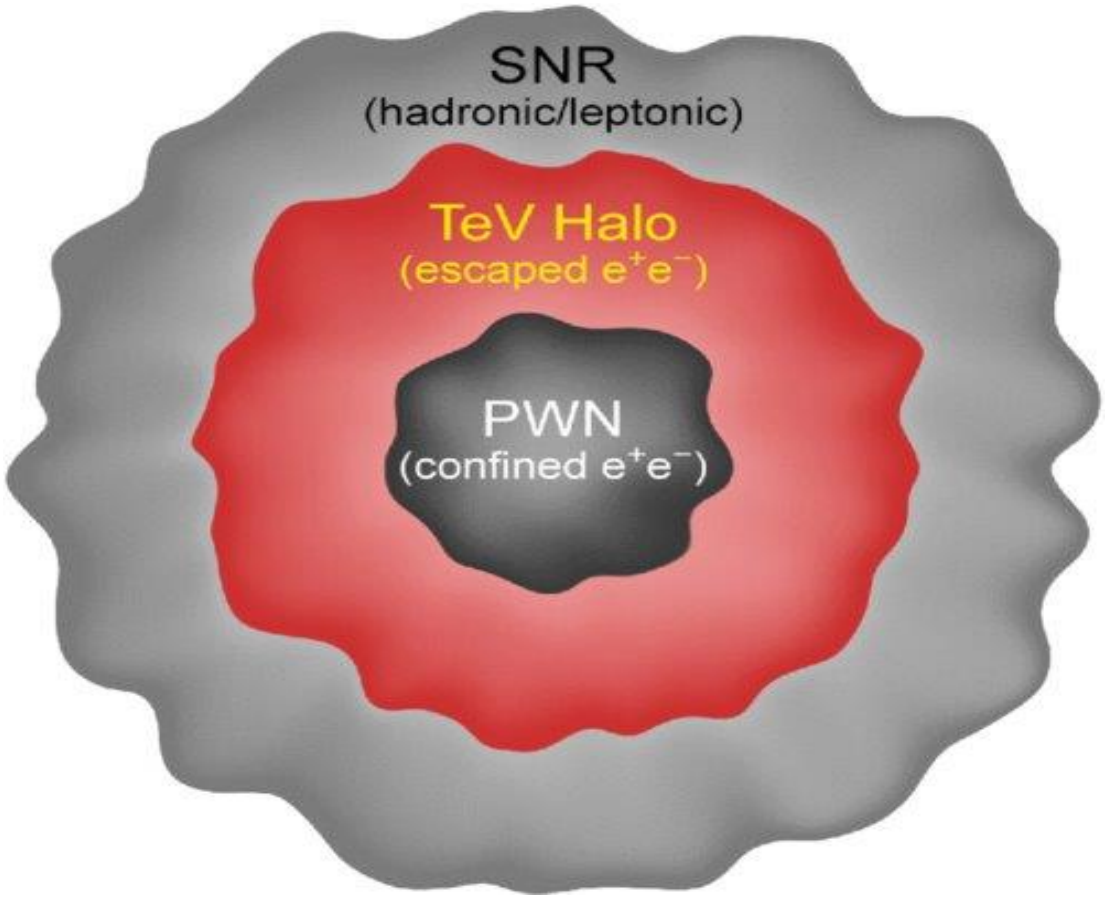

Sudoh, T., Linden, T., Beacom, J. (2019) *Feynman Diagram of Neutral Pion Decay*. arXiv:2502.18384

TeV Halos

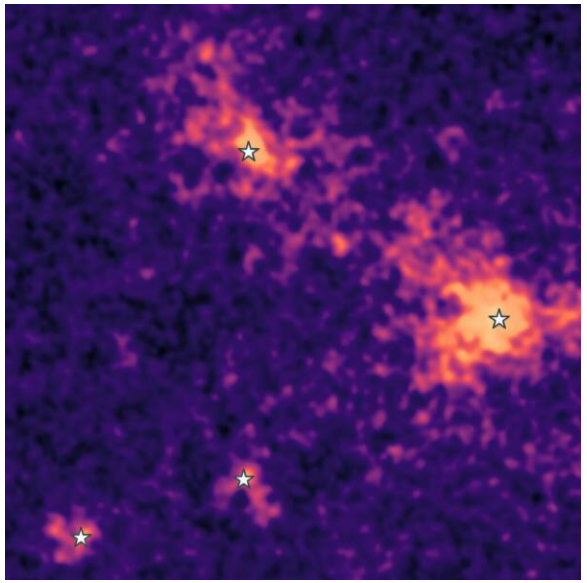

Coutiño, S. (2023). *HAWC significance map of some of TeV halos included in the analysis (marked with white stars).*

Contribute to diffuse glow?

The combined, overlapping glow from thousands of unresolved TeV halos throughout the galaxy could be a significant contributor to the diffuse gamma-ray background that LHAASO is measuring

The Gamma-Ray Eye: LHAASO

Large High Altitude Air Shower Observatory (Daocheng, China)

Designed for cosmic-ray and γ-ray studies at TeV and PeV energies

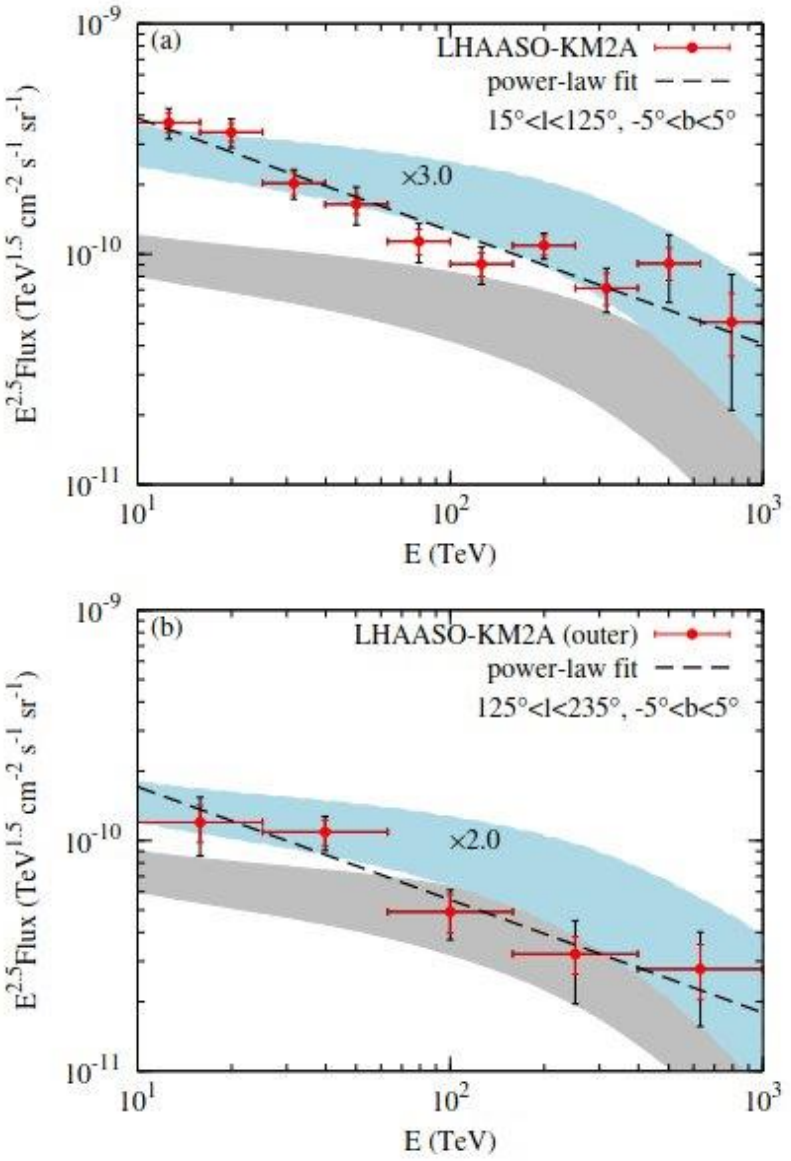

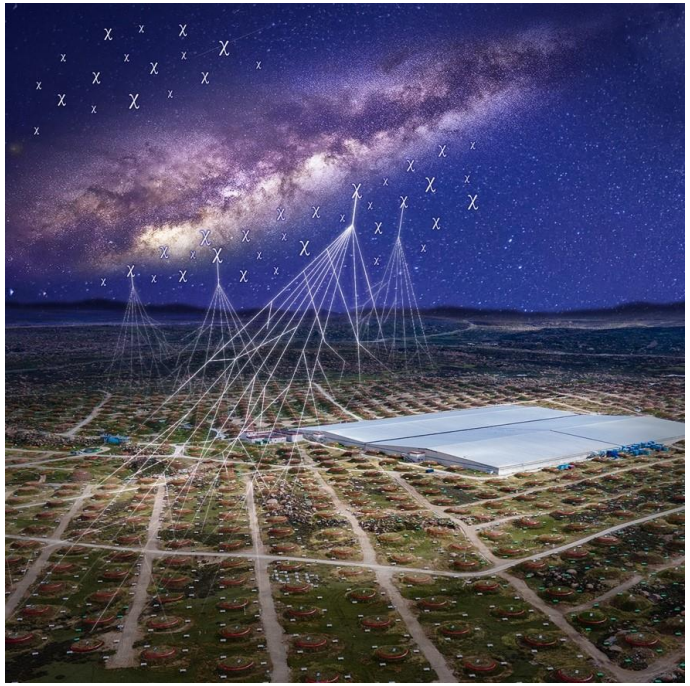

LHAASO (2022). *Artist rendition of cosmic rays being detected at LHAASO.*

LHAASO Collaboration (2023). *Measured fluxes of diffuse γ-ray emission in the inner and outer Galaxy regions.* arXiv:2305.05372v2

Points directly to source

Difficult to detect due to neutral charge and small cross section

Neutrinos

Produced through hadronic interactions (smoking gun!)

Should approximately parallel gamma-ray emission in high energies in pion 1:1:1 ratio

$$\pi^+ \rightarrow \mu^+ + \nu_\mu \rightarrow e^+ \bar{\nu}_\mu \nu_e \nu_\mu,$$
$$\pi^- \rightarrow \mu^- + \bar{\nu}_\mu \rightarrow e^- \nu_\mu \bar{\nu}_e \bar{\nu}_\mu$$

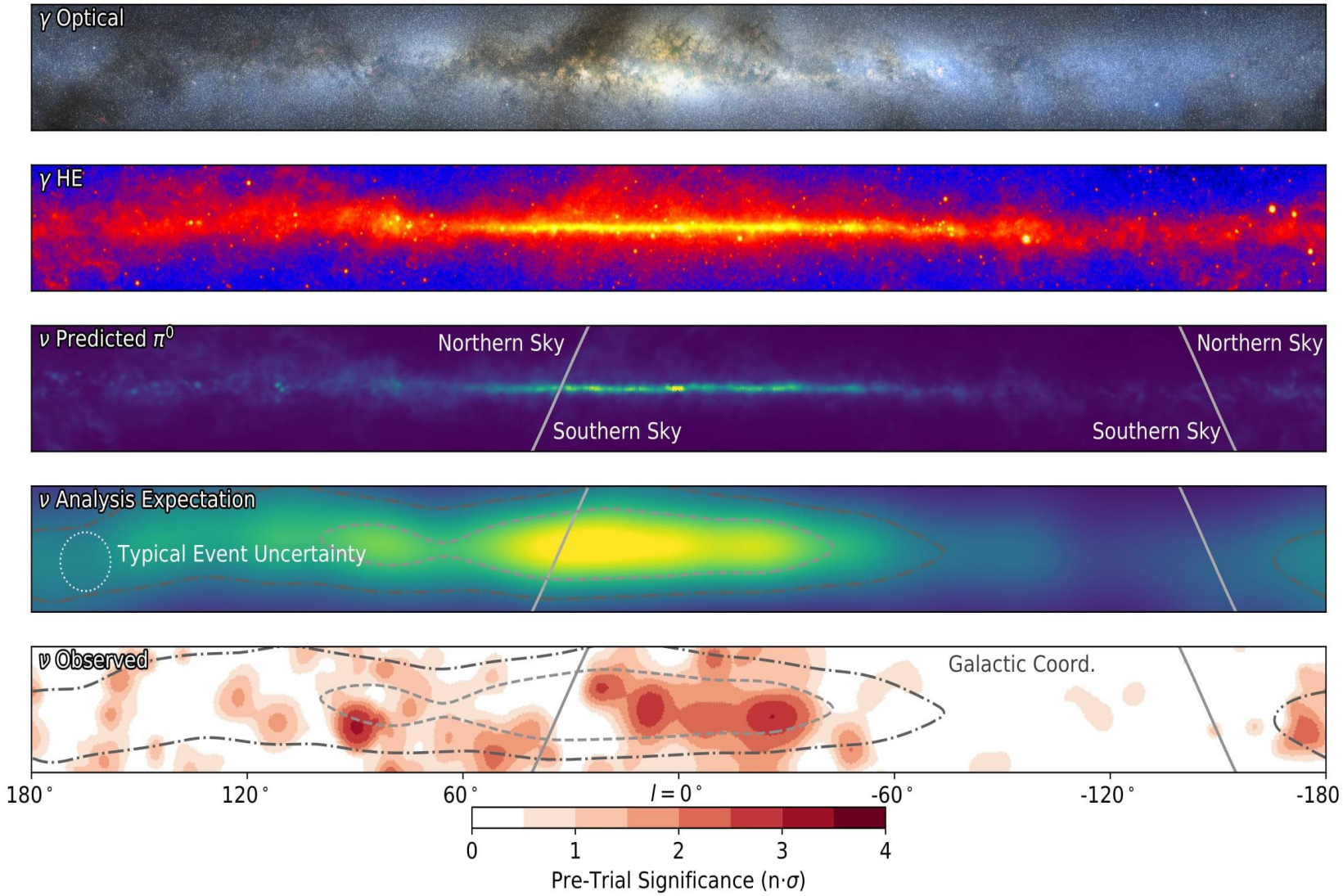

IceCube Collaboration. (2023). *Observation of high-energy neutrinos from the Galactic plane*. Science.

The Neutrino Eye: IceCube

Cubic-kilometer neutrino telescope at the geographic South Pole

Digital Optical Modules detect Cherekov light from charged lepton resulting from neutrino-ice interaction

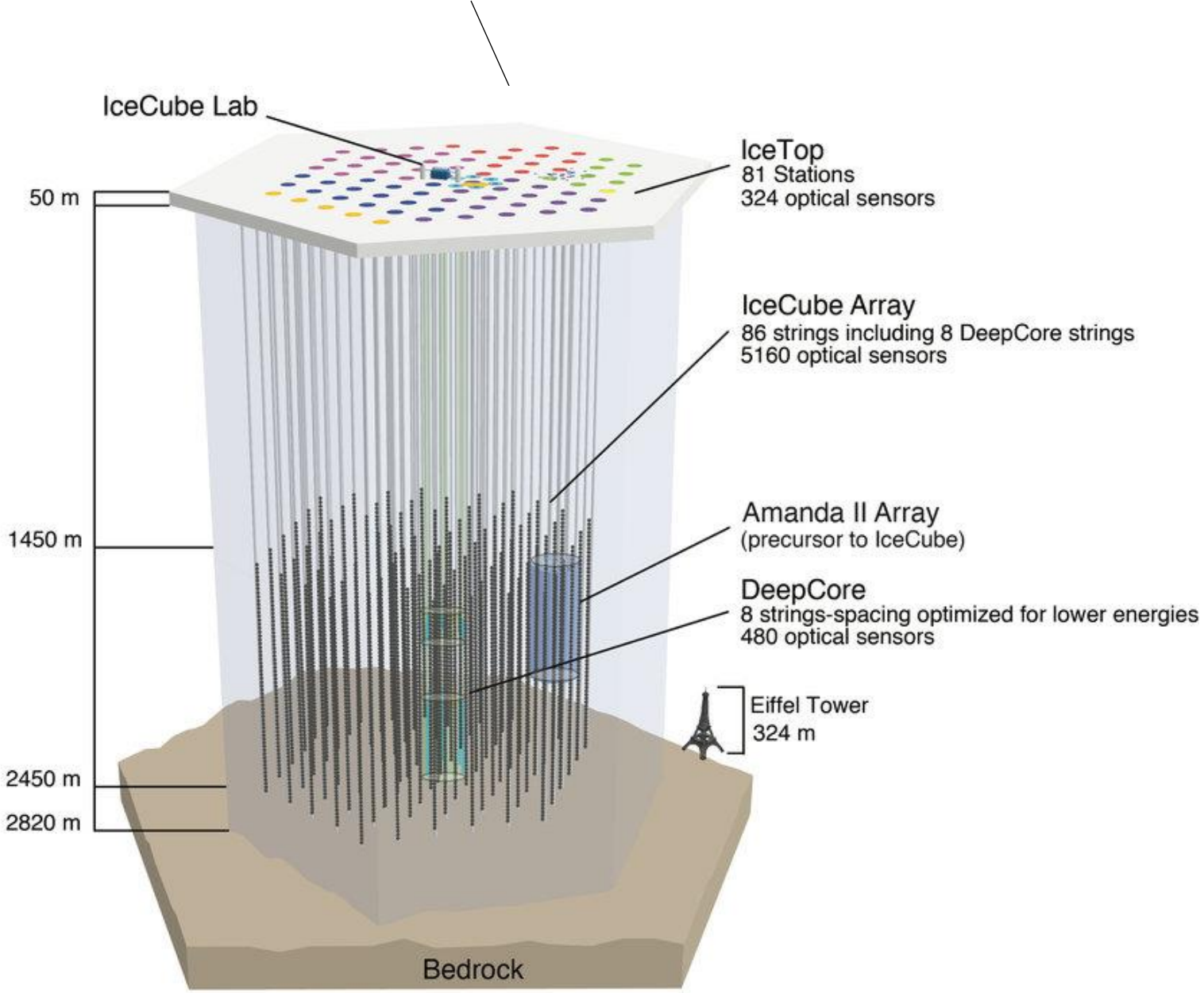

Karen Andeen and Matthias Plum for the IceCube Collaboration. (2019). *Three-dimensional layout of the neutrino detector.*

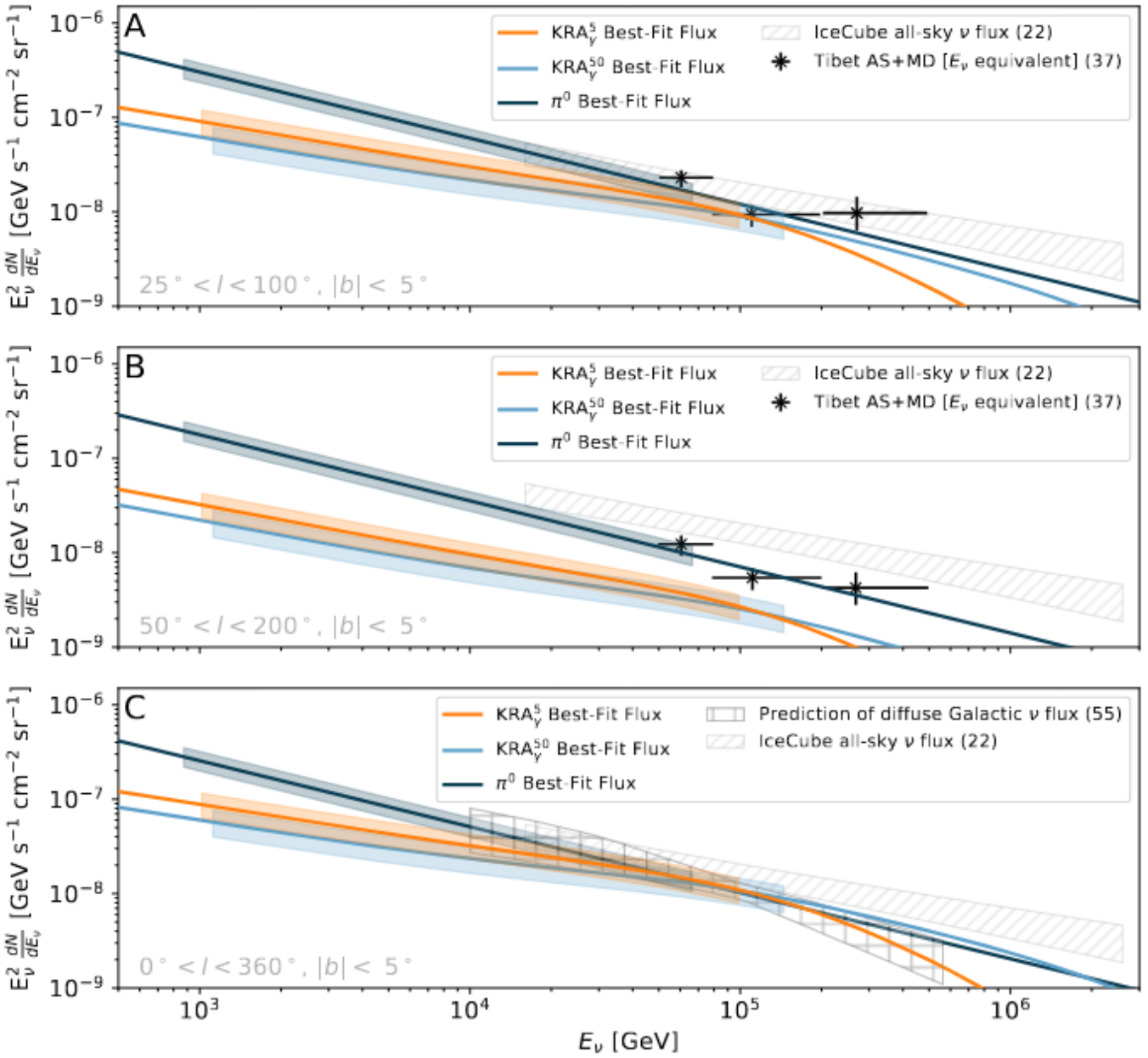

IceCube Collaboration. (2023). *Observation of high-energy neutrinos from the Galactic plane.* Science.

The Neutrino Eye: IceCube

Cubic-kilometer neutrino telescope at the South Pole

Digital Optical Modules (DOMs) detect Cherekov light from charged lepton resulting from neutrino-ice interaction

π^0: spatial probability template based on gamma-ray emission

KRA_γ^5: constant, model-averaged spectrum over the sky with 5 PeV cosmic-ray energy cutoff

KRA_γ^{50}: 50 PeV cosmic-ray energy cutoff

RESULTS

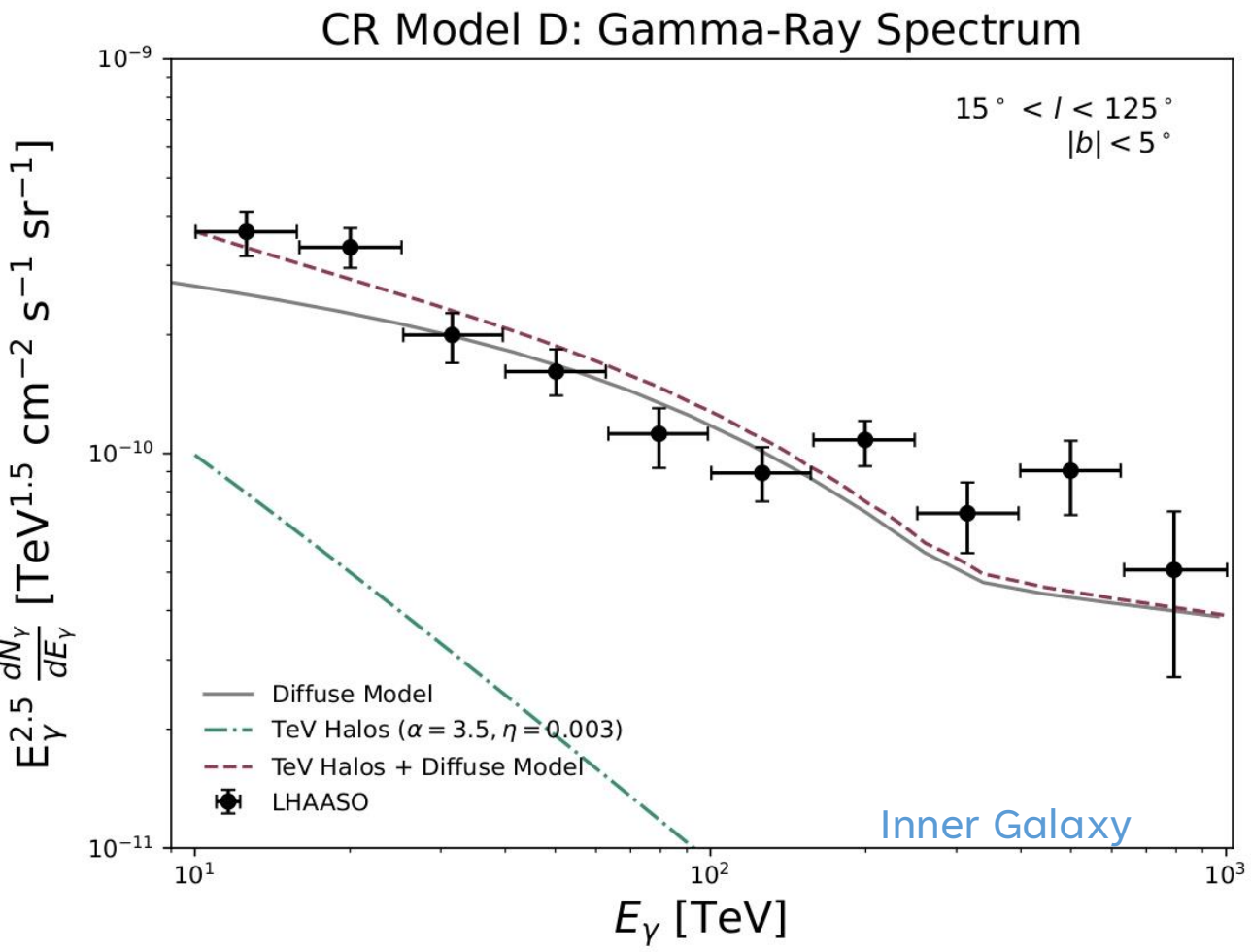

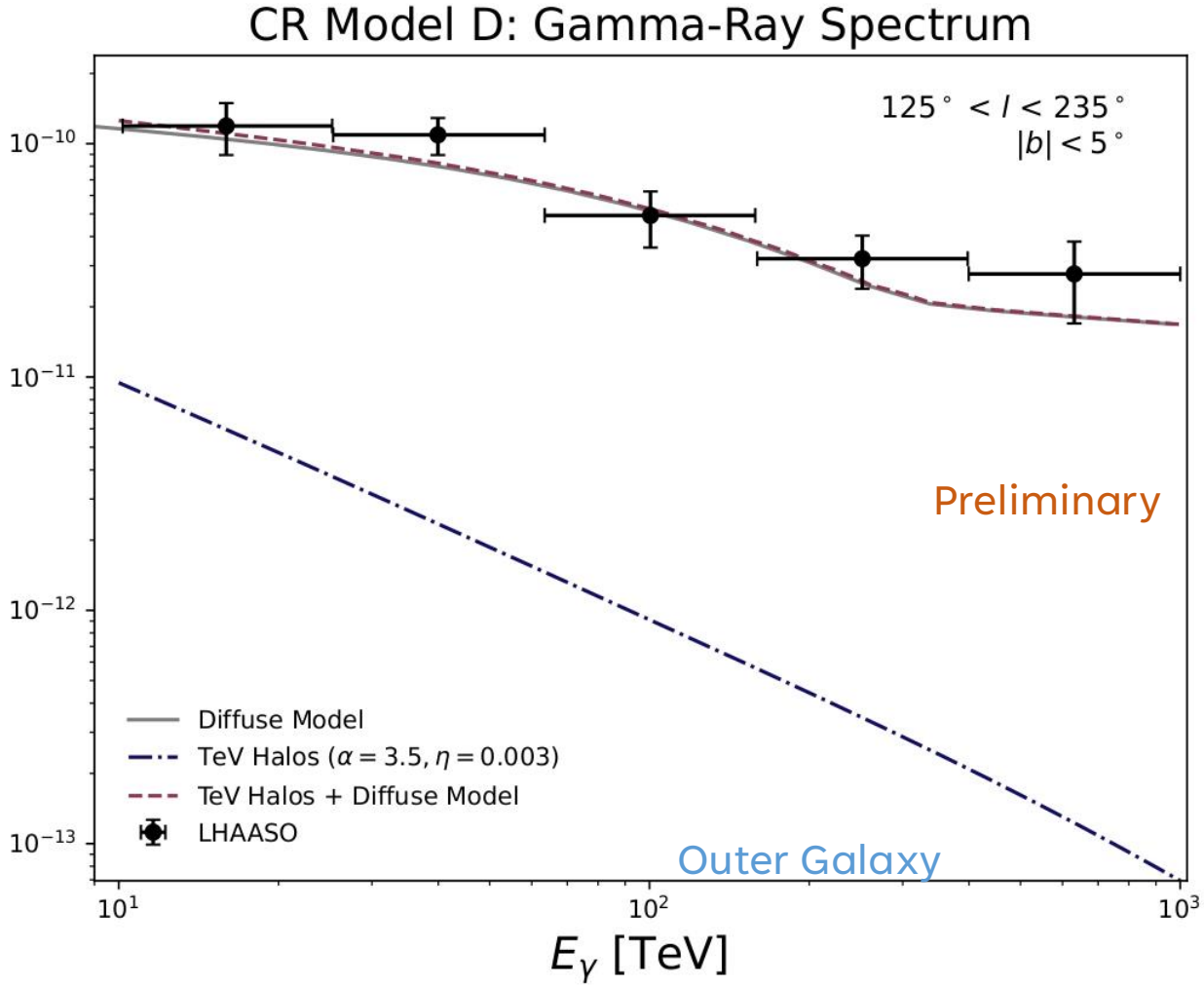

Diffuse model makes up majority of data

- Limited TeV halo contribution at all energies

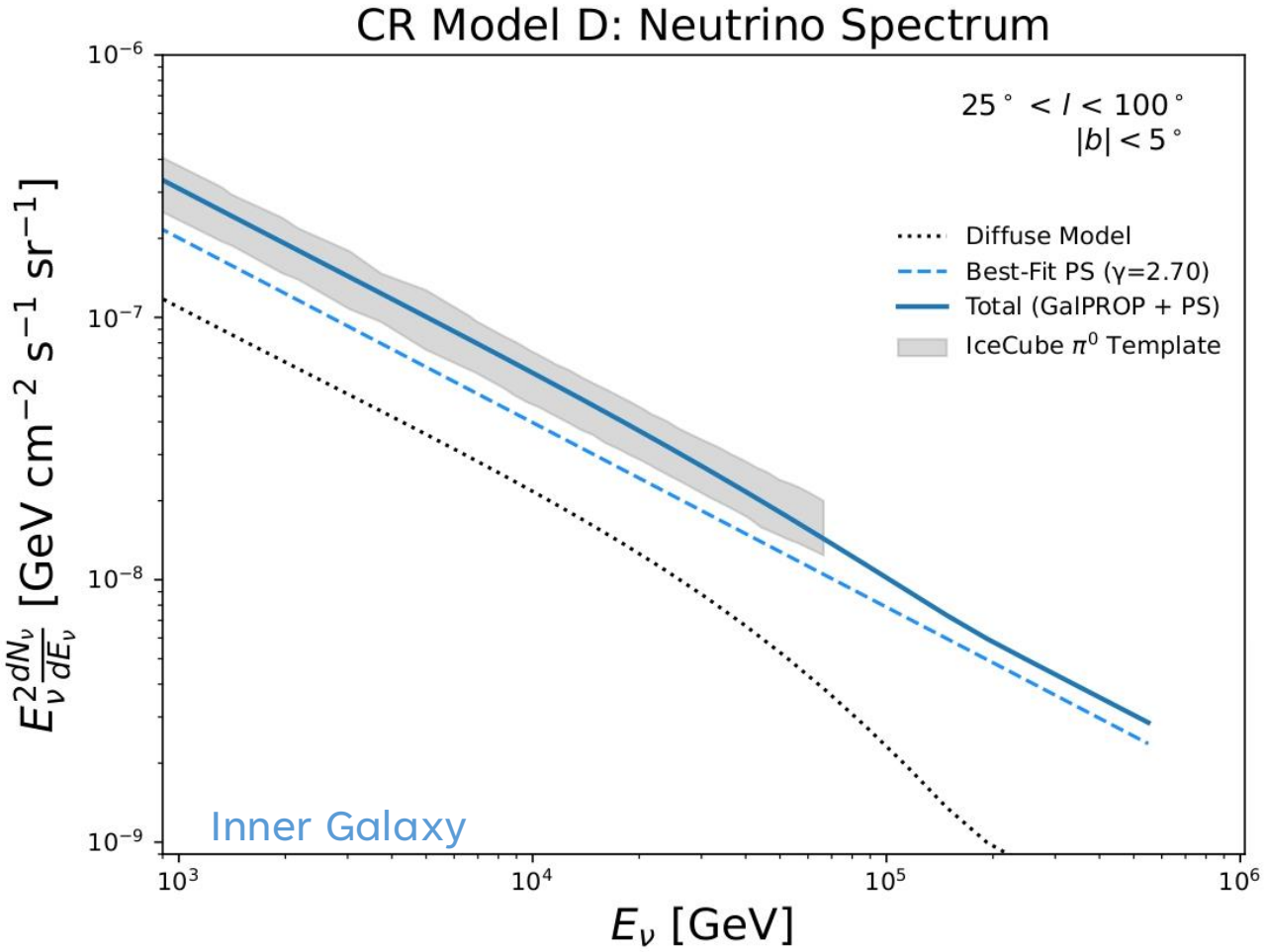

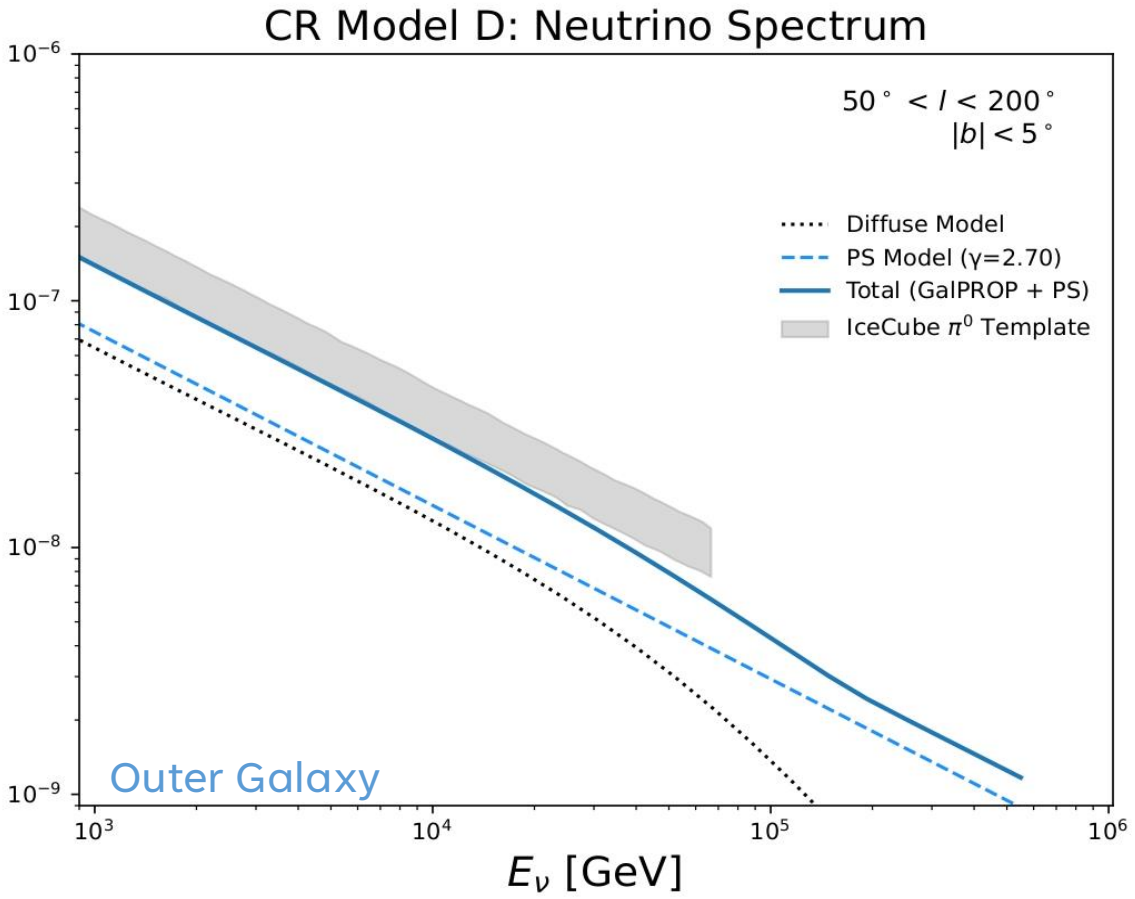

Neutrino point sources account for more than half of emission seen by IceCube

Parameter Landscape

Preliminary

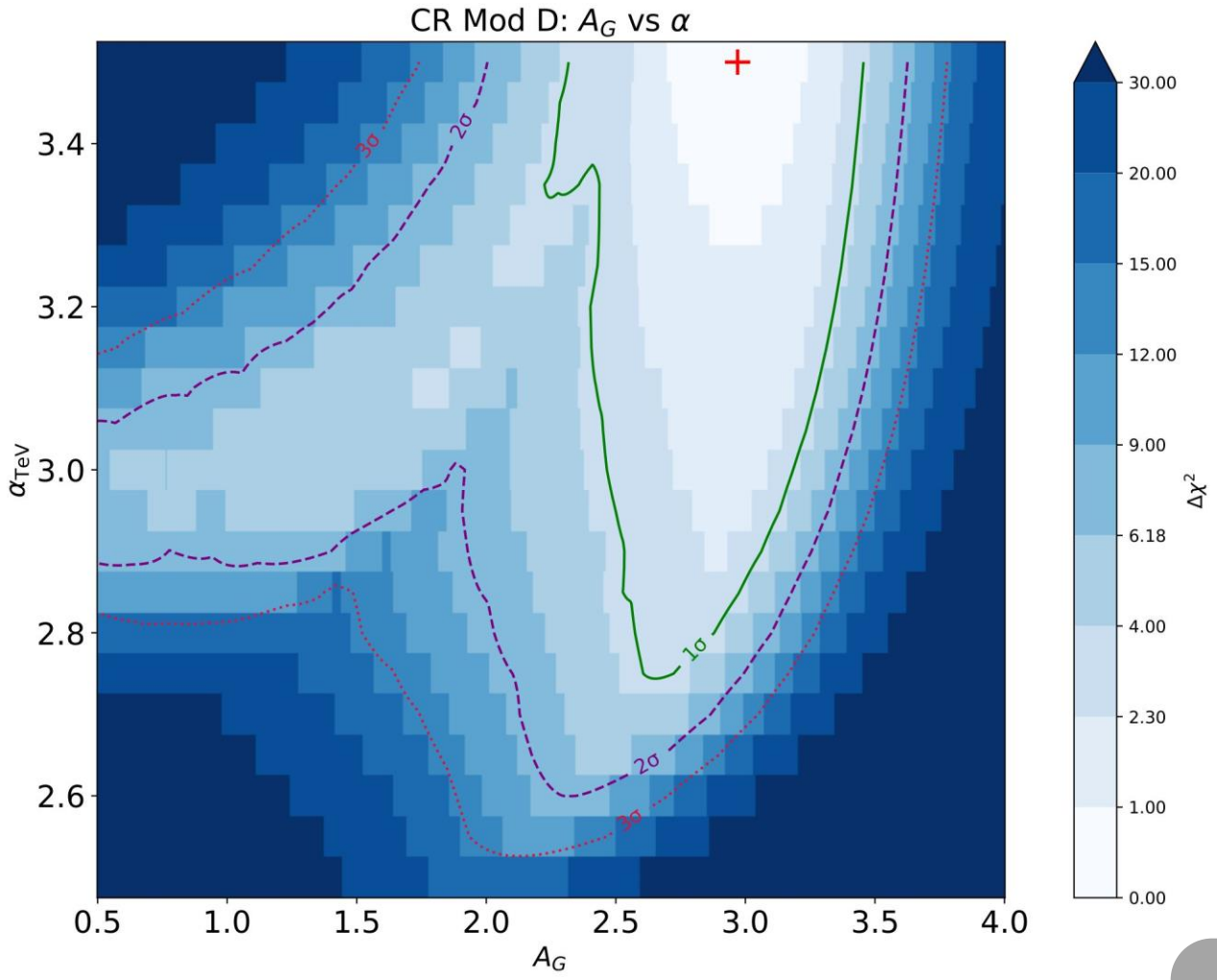

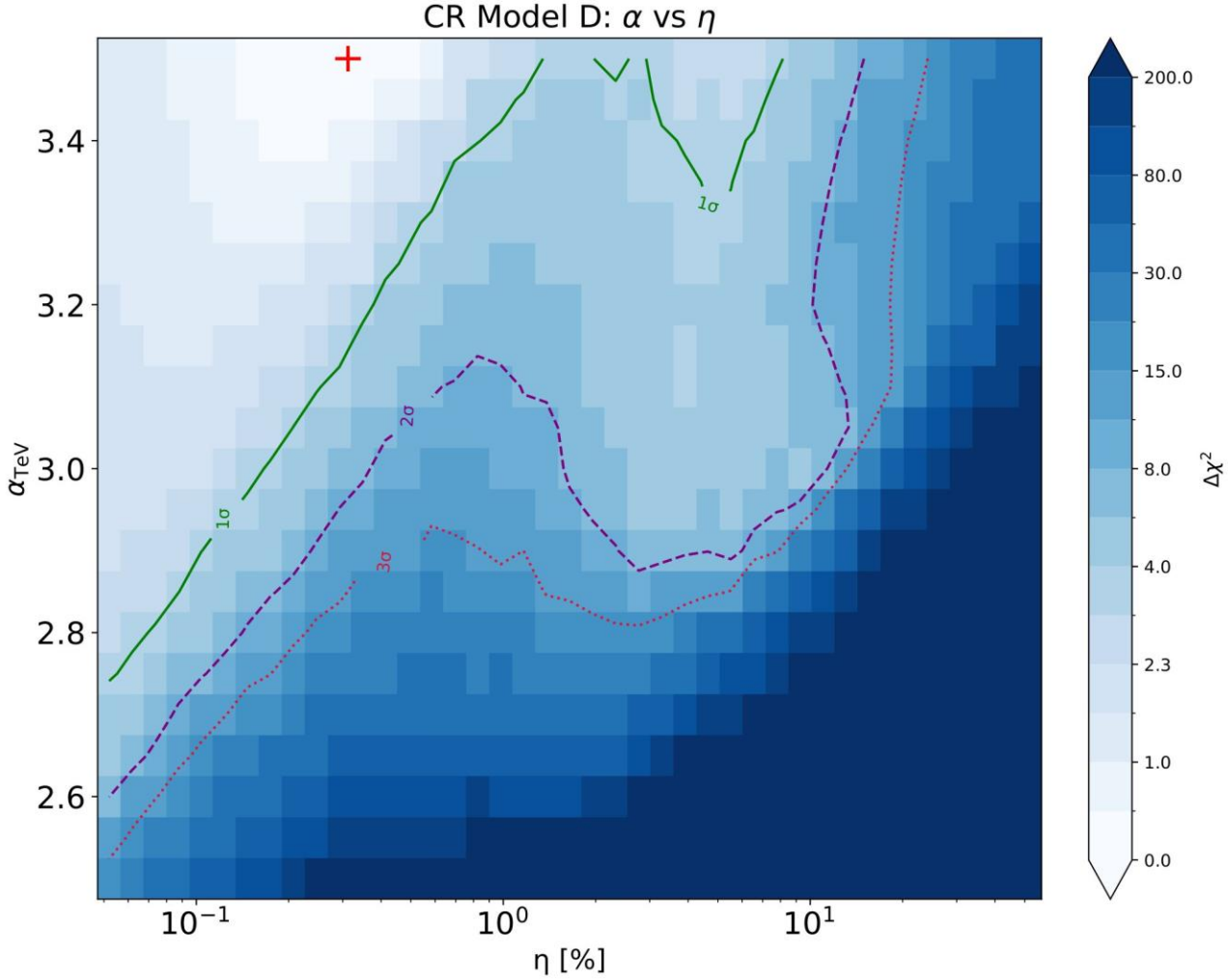

TeV halos possess soft spectra of $3.0 \lesssim \alpha \leq 3.5$, with averaged efficiency η up to roughly 10% within 1σ

CONCLUSION

- **A multi-messenger framework** to combine baseline cosmic-ray models, new source populations like TeV Halos and Point Source models, and observational data from LHAASO and IceCube

- Our results across six CR models demonstrate the following:
  - In gamma-ray channel, the LHAASO flux is primarily recovered by the diffuse hadronic model, leaving a subdominant role for unresolved leptonic TeV halos
  - From lack of a dominant leptonic component, it follows that more than half of the IceCube emission is attributed to hadronic point sources rather than being 'diluted' by a large leptonic background

QUESTIONS?

Thank you!

BACKUP SLIDES

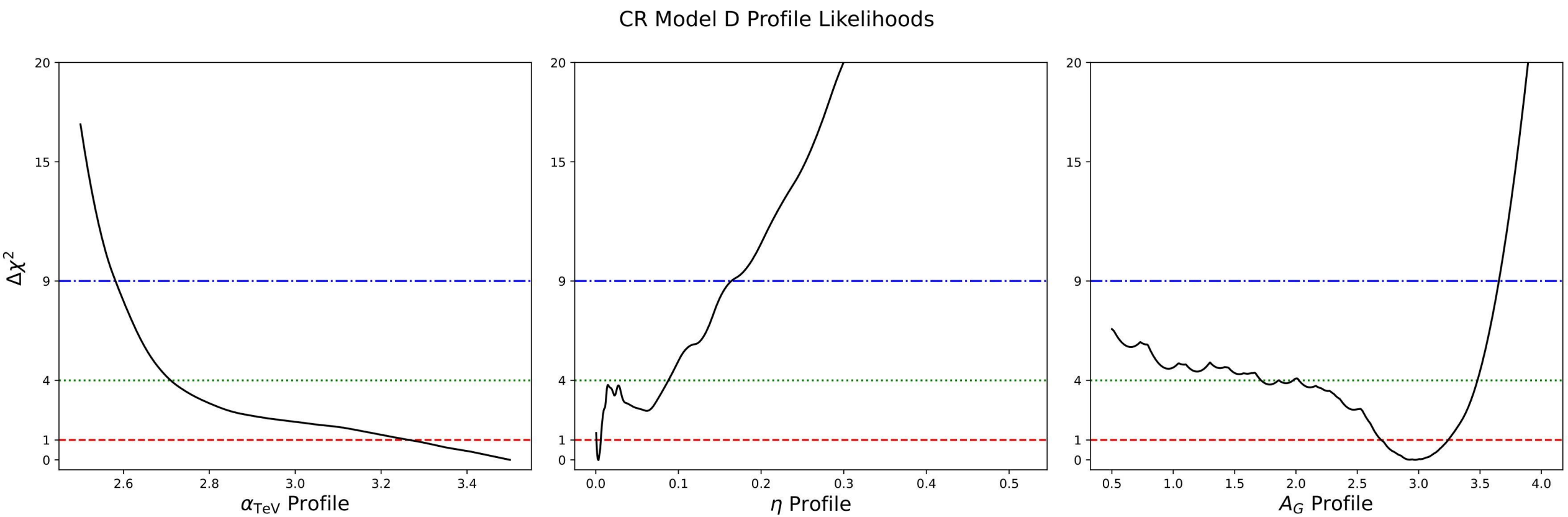
CR Model D Profile Likelihoods
$\Delta\chi^2$
20
15
9
4
1
0
2.6
2.8
3.0
3.2
3.4
α_{TeV} Profile
0.0
0.1
0.2
0.3
0.4
0.5
η Profile
0.5
1.0
1.5
2.0
2.5
3.0
3.5
4.0
A_G Profile

ALTERNATE COSMIC RAY MODEL (E)

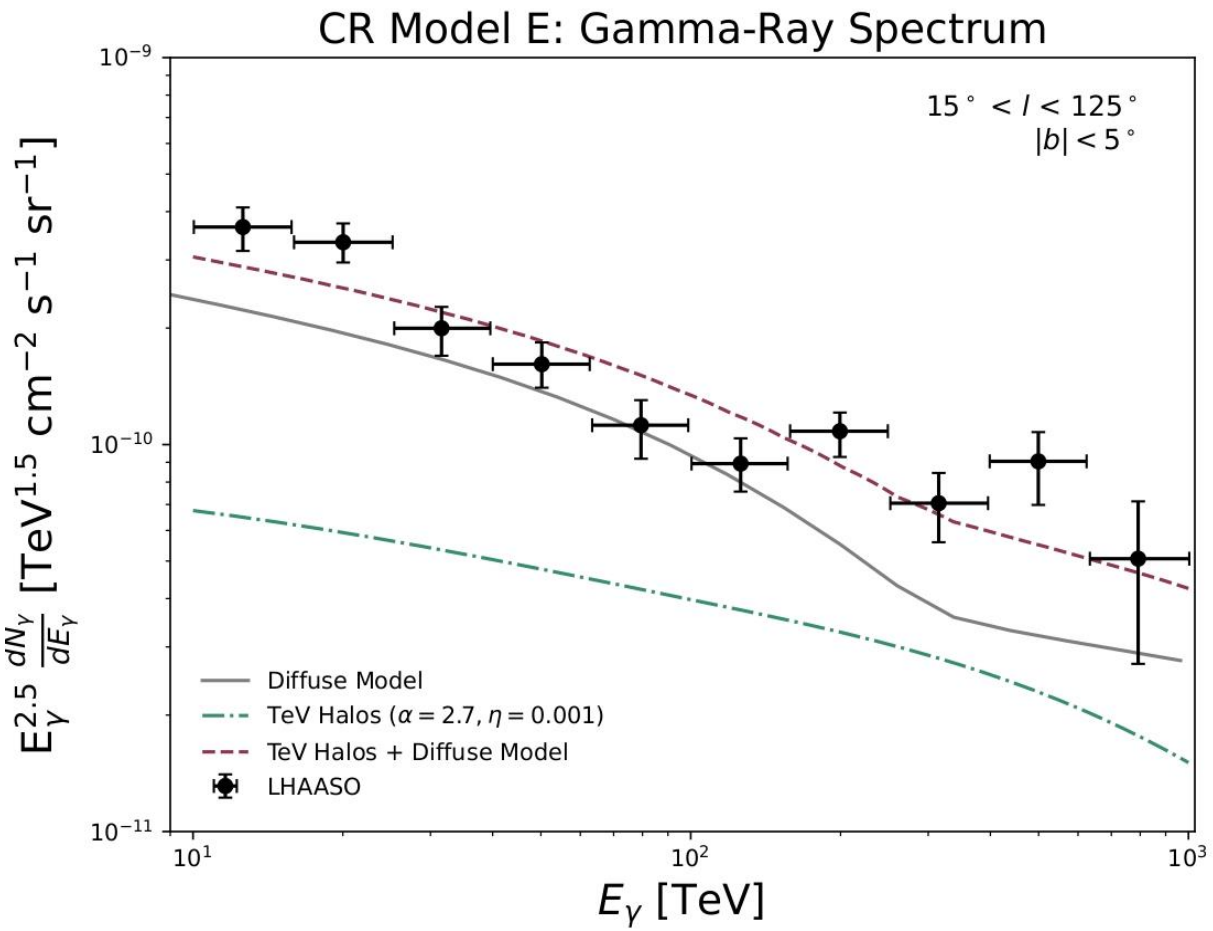

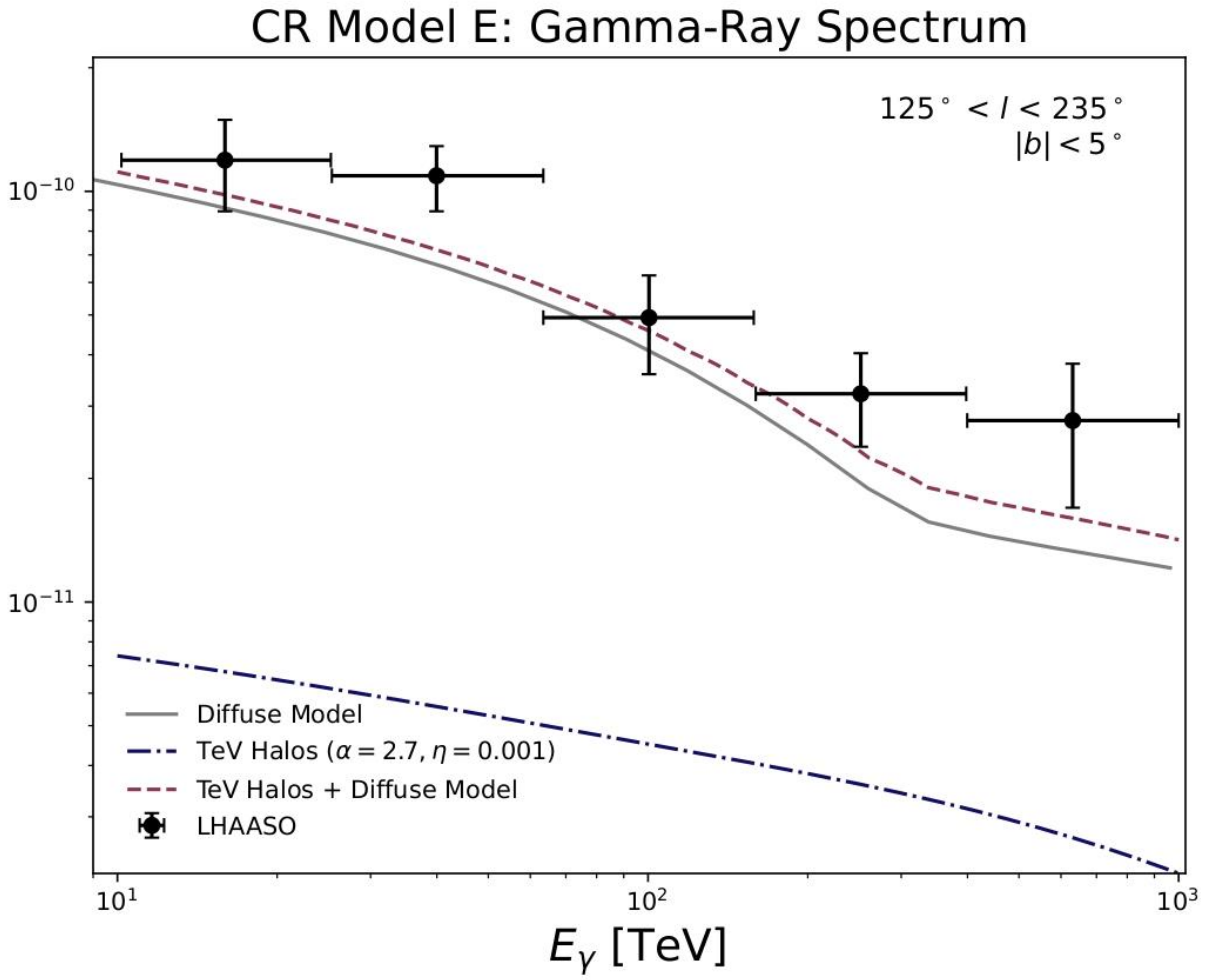

Harder spectral index of TeV halo at higher energies; suggests that model E fits the shape of the LHAASO data

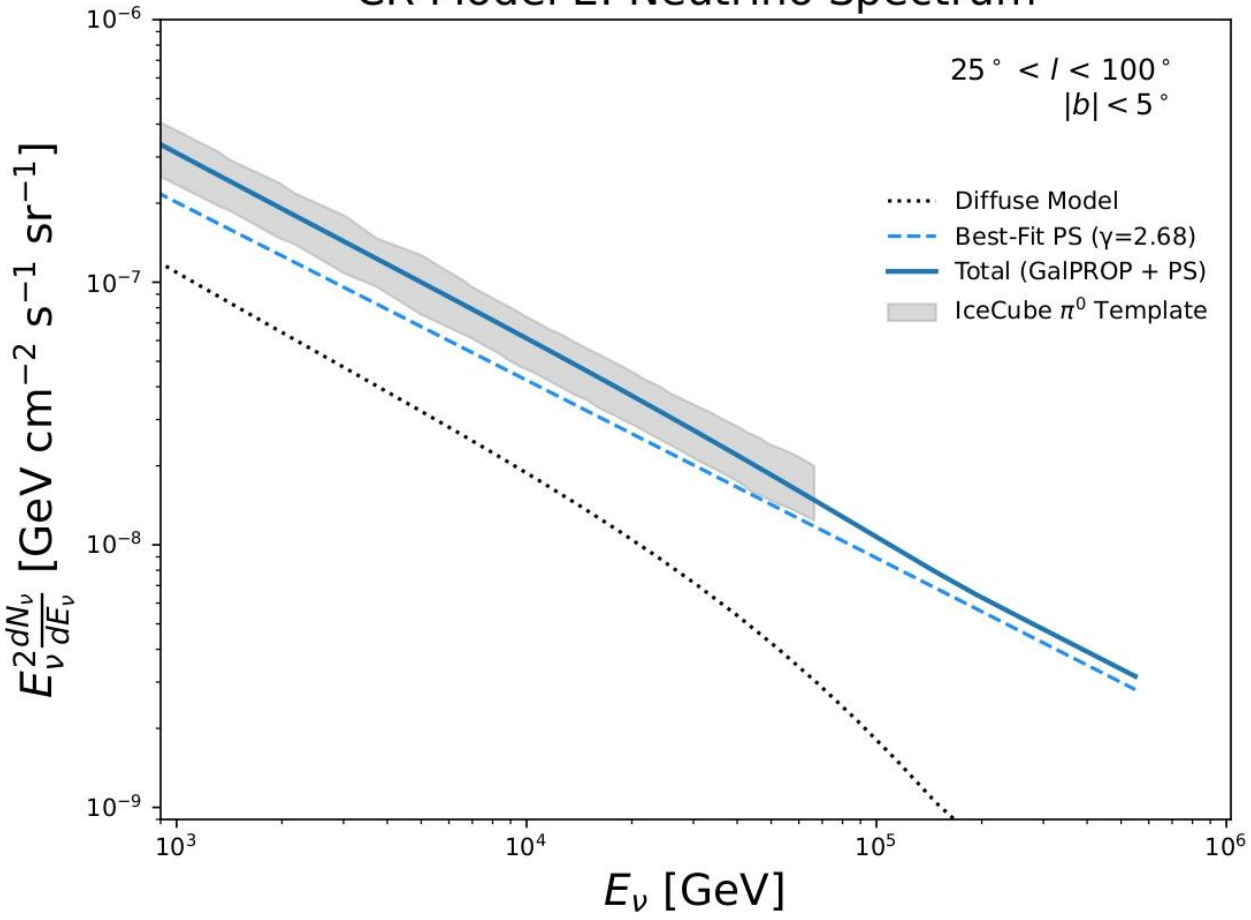

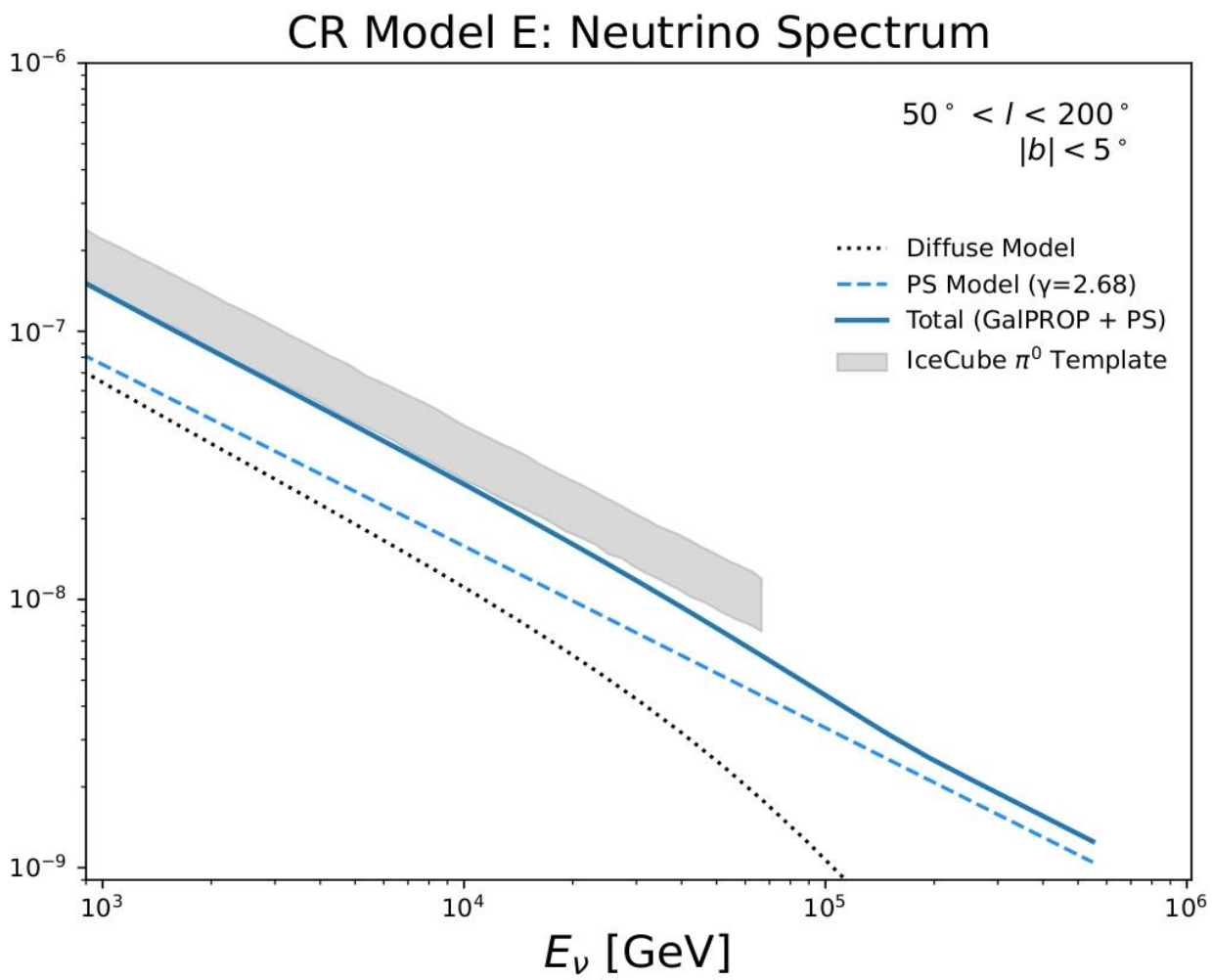

Still: Neutrino point sources account more than half of emission seen by IceCube

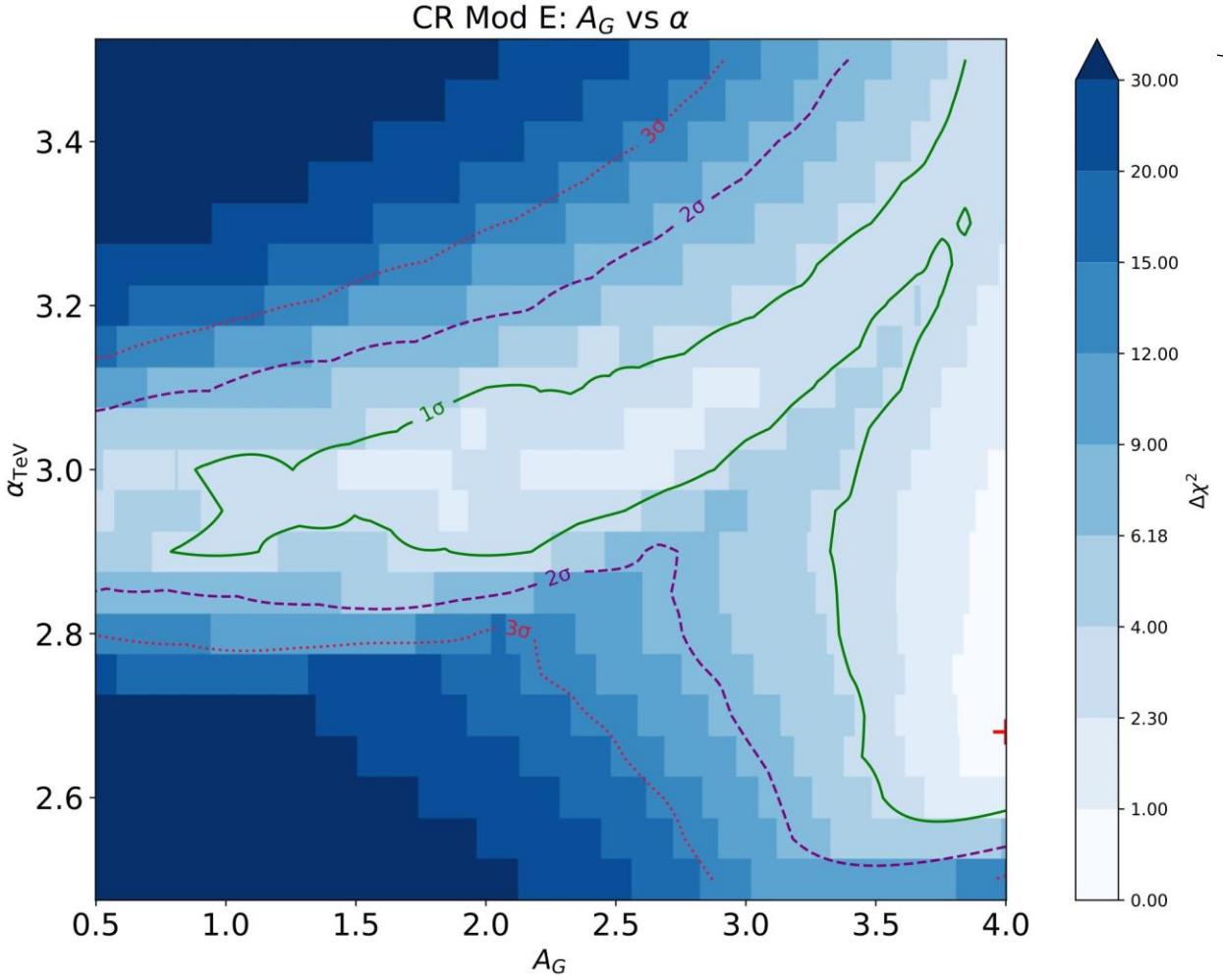

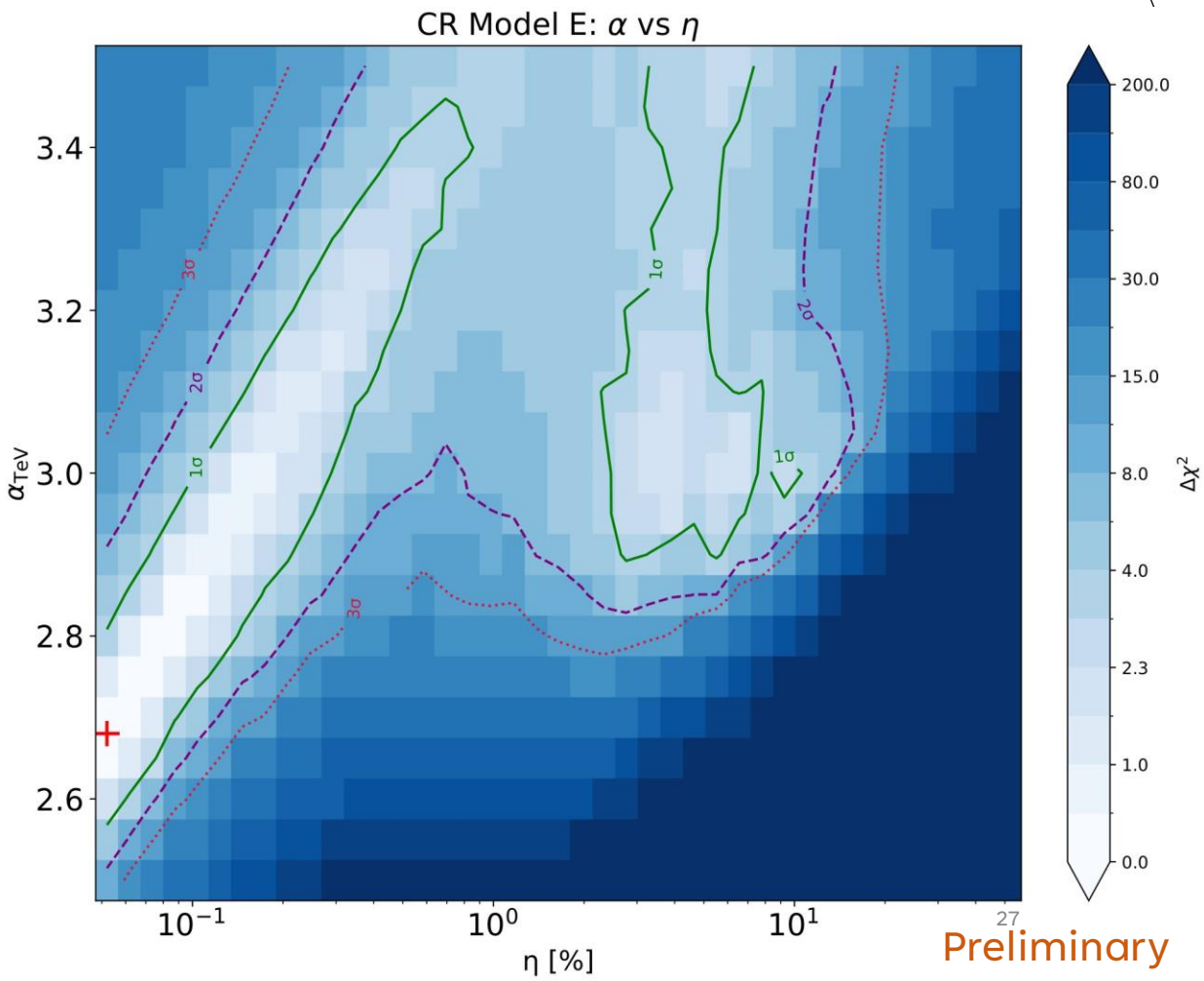

Preliminary

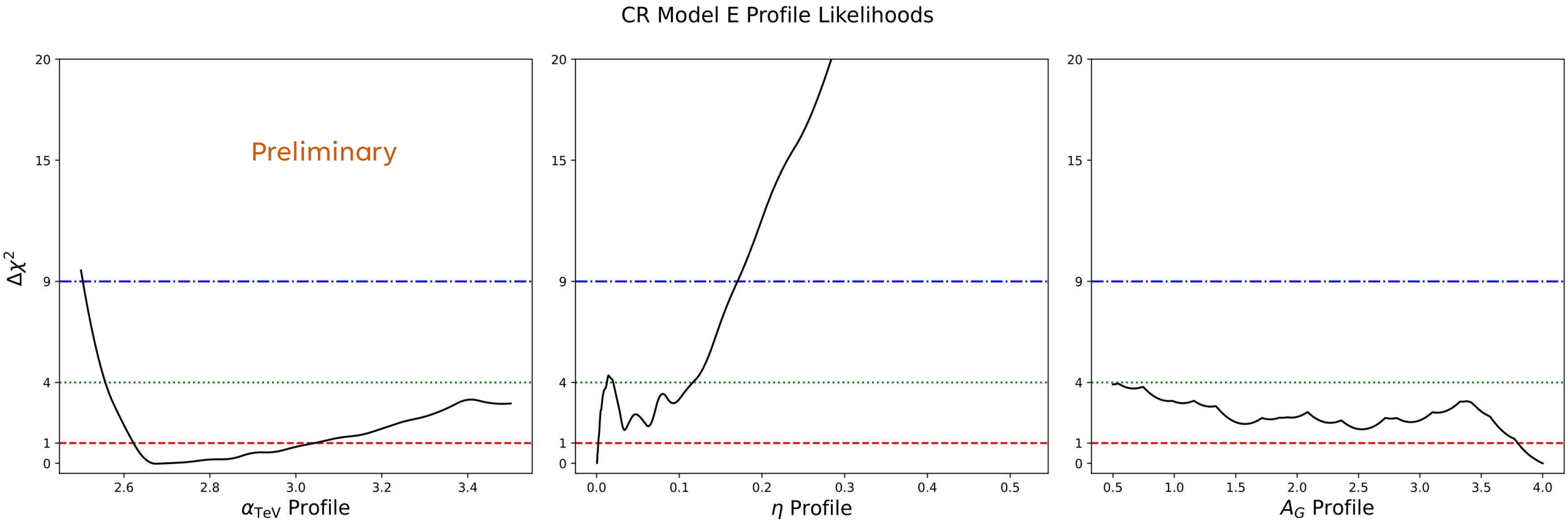
CR Model E Profile Likelihoods
Preliminary
$\Delta\chi^2$
α_{TeV} Profile
η Profile
A_G Profile

arxiv:2112.09706

CR Model	δ	z_L (kpc)	$D_0 \times 10^{28}$ (cm^2/s)	v_A (km/s)	$dv_c/d\|z\|$ (km/s/kpc)	α_1 H/He	R_{br_1} H/He (GV)	α_2 H/He	R_{br_2} H/He (GV)	α_3 H/He
A	0.33	5.7	6.70	30.0	0	1.74/1.70	6.0/7.4	2.04/2.16	14.0/21.5	2.41/2.39
B	0.37	5.5	5.50	30.0	2	1.72/1.74	6.0/8.0	2.00/2.14	12.4/21.0	2.38/2.375
C	0.40	5.6	4.85	24.0	1	1.69/1.65	6.0/6.7	2.00/2.13	12.4/20	2.38/2.355
D	0.45	5.7	3.90	24.0	5.5	1.69/1.68	6.0/7.0	1.99/2.12	12.4/18.7	2.355/2.34
E	0.50	6.0	3.10	23.0	9	1.71/1.68	6.0/7.2	2.02/2.14	11.2/17.5	2.38/2.33
F	0.43	3.0	1.85	20.0	2	1.68/1.74	6.0/10.5	2.08/2.09	13.0/21.0	2.41/2.33

TABLE I. The cosmic-ray propagation assumptions (CR Model), determined by the diffusion index δ, the diffusion scale height z_L, the normalization of the diffusion co-efficient D_0, the Alfvén velocity v_A, the galactic convection gradient dv_c/dv, the injection indices α_1, α_2, α_3, and the rigidity breaks R_{br_1} and R_{br_2} for cosmic-ray hydrogen and helium isotopes. In the last five columns, the first values refer to hydrogen injection properties and the second values to helium.

Working Assumptions:
assume isotropic and homogeneous diffusion in the medium outside the TeV Halo regions

Evaluated in GALPROP for any direction by integrating along our line of sight the emissivity per nucleon multiplied with the expected ISM gas density

Model	GALPROP Normalization A_G	TeV Halo η (%)	$\alpha_{\rm TeV}$	χ^2_γ	ν PS $A_{\rm PS}$	$\gamma_{\rm PS}$	$\chi^2_{\nu,\rm inner}$	$\chi^2_{\nu,\rm outer}$	$\chi^2_{\nu,\rm full}$	Total $\sum\chi^2$
A	$1.62^{+0.35}_{-0.12}$	$6.4^{+2.4}_{-6.1}\%$	$3.50^{+0.00}_{-0.11}$	22.06	$8.31^{+6.34}_{-4.26}\times10^{-9}$	$2.73^{+0.21}_{-0.21}$	2.16×10^{-4}	3.07	1.29	25.13
B	$1.98^{+0.19}_{-0.30}$	$0.5^{+7.0}_{-0.3}\%$	$3.50^{+0.00}_{-0.13}$	23.50	$7.86^{+6.39}_{-4.24}\times10^{-9}$	$2.73^{+0.22}_{-0.23}$	2.11×10^{-4}	2.69	1.08	26.19
C	$2.55^{+0.20}_{-0.25}$	$0.4^{+0.4}_{-0.2}\%$	$3.50^{+0.00}_{-0.16}$	23.48	$7.86^{+6.59}_{-4.34}\times10^{-9}$	$2.71^{+0.23}_{-0.23}$	1.96×10^{-6}	2.55	1.02	26.03
D	$2.97^{+0.27}_{-0.27}$	$0.3^{+0.3}_{-0.2}\%$	$3.50^{+0.00}_{-0.23}$	25.41	$7.86^{+6.99}_{-4.39}\times10^{-9}$	$2.70^{+0.24}_{-0.25}$	1.36×10^{-4}	2.39	0.94	27.79
E	$4.00^{+0.00}_{-0.20}$	$0.1^{+0.1}_{-0.0}\%$	$2.68^{+0.36}_{-0.06}$	28.37	$8.91^{+7.24}_{-4.69}\times10^{-9}$	$2.68^{+0.22}_{-0.24}$	7.10×10^{-5}	2.62	1.06	30.99
E'	$5.08^{+0.45}_{-0.78}$	$0.2^{+0.2}_{-0.1}\%$	$3.50^{+0.00}_{-0.77}$	26.30	$8.20^{+7.72}_{-4.72}\times10^{-9}$	$2.66^{+0.26}_{-0.28}$	2.06×10^{-5}	2.06	0.80	28.36
F	$3.72^{+0.28}_{-0.31}$	$0.3^{+0.3}_{-0.2}\%$	$3.50^{+0.00}_{-0.18}$	22.24	$8.08^{+6.98}_{-4.46}\times10^{-9}$	$2.70^{+0.24}_{-0.25}$	1.87×10^{-4}	2.57	0.93	24.81

TeV halos possess soft spectra of $3.0 \lesssim \alpha \leq 3.5$, with averaged efficiency η up to roughly 10% within 1σ

With higher AG limit, there is dominant diffuse emission, which makes the emission from the TeV halos prefer $\alpha \simeq 3.5$.

TeV Halos

Explain the Positron Excess?

For years, satellites (Pamela, AMS) detected more high-energy positrons near Earth than our standard models can explain.

TeV halos, acting as local factories for positrons, could explain this anomaly (Dekker, A., Holst, I., Simon, E. et al., 2024, arxiv:2306.00051)

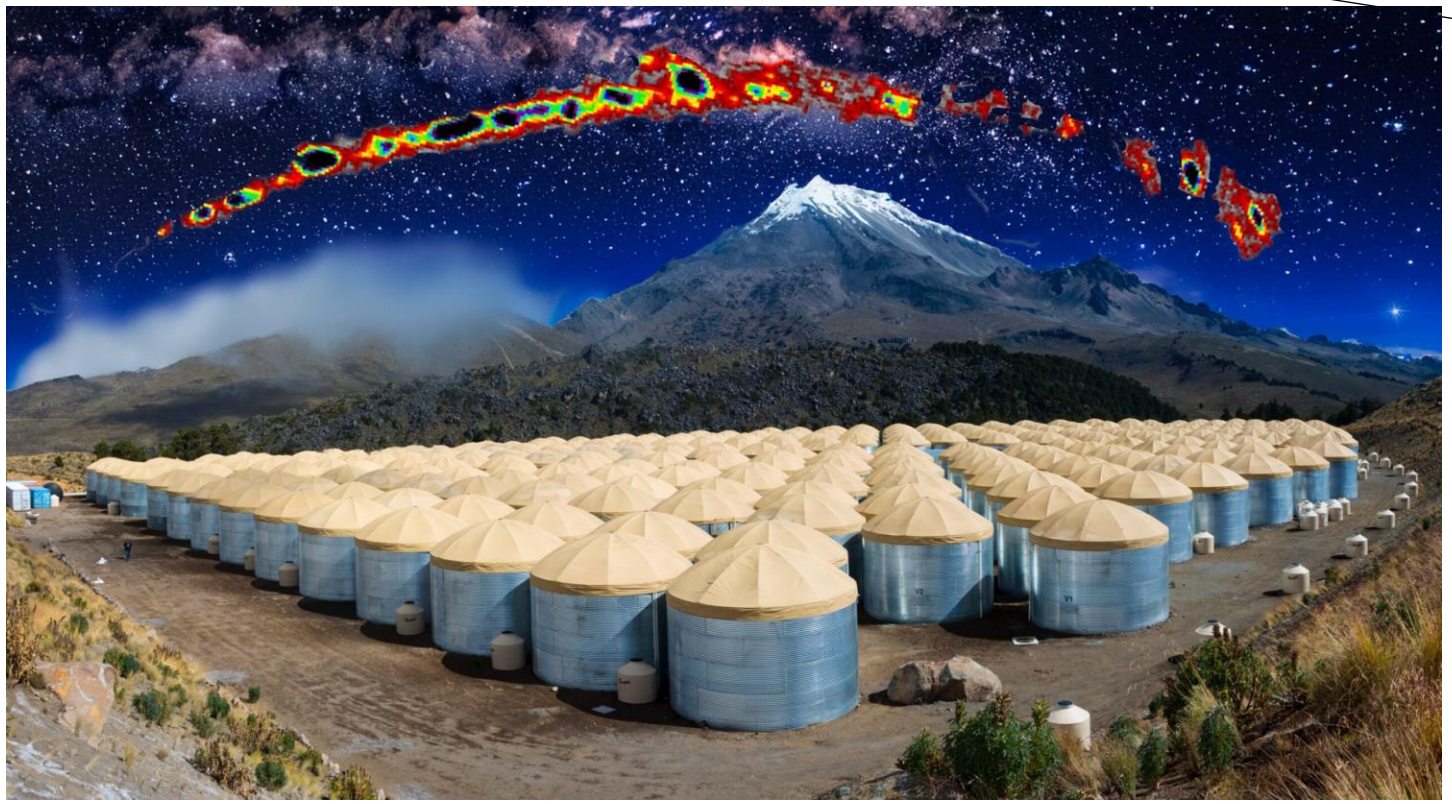

Goodman, J. (2023). *HAWC site with superposition of Milky Way's plane as seen in gamma-rays*